Unclassified

Technical Report No. 6

MECHANICAL CHARACTERIZATION OF SOLITHANE 113

by

M. G. Sharma and Y. S. Lee

JPL Contract No. 950875

This work was performed for the Jet Propulsion Laboratory, California Institute of Technology, sponsored by the National Aeronautics and Space Administration under Contract NAS 7-100

The Pennsylvania State University

University Park, Pennsylvania

November 1968

MECHANICAL CHARACTERIZATION OF SOLITHANE 113

by

M. G. Sharma and Y. S. Lee

JPL Contract No. 950875

This work was performed for the Jet Propulsion Laboratory, California Institute of Technology, sponsored by the National Aeronautics and Space Administration under Contract NAS 7-100

The Pennsylvania State University

University Park, Pennsylvania

November 1968

Preface

This is the sixth technical report covering the research work under the project entitled, "A test Program to Determine the Mechanical Behavior of Solid Propellants". The work reported here particularly refers to the study of mechanical behavior of Solithane 113 under biaxial loading at room temperature conditions. From the experimental data the strain energy function for the material has been determined.

Abstract

The report describes two types of biaxial stress experiments to characterize Solithane 113 corresponding to time independent mechanical behavior. The first type of experimentswas conducted under controlled strain rates and the second under controlled stress rates. A method has been described in this report to obtain the strain energy function for the material from the biaxial experimental results that included time effects.

Results indicate that Solithane 113 after it reaches mechanical equilibrium can be characterized by a simple strain energy function that follows from the well known kinetic theory of rubber elasticity.

Mechanical Characterization of Solithane 113

Introduction

Rubberlike materials display large deformation under external loading conditions leading to nonlinearity between stress and strain. Solithane 113 under room temperature conditions behaves like a rubberlike material and displays about 50 percent elongation as shown by the stress-strain curve in Fig. 1. The mechanical behavior of the material under such conditions is usually better described by a strain energy function characteristic of the material. The determination of a strain energy function is generally complicated by the time dependency of the material behavior.

A method has been described in this report, which makes it possible to determine the strain energy function for the material corresponding to its equilibrium behavior.

Experimental Investigation

The Material and Specimen Preparation

The material used in the experimental program is a polyurethane elastomer obtained by combining Solithane 113 with DB castor oil. Solithane 113 is a polyether based liquid urethane prepolymer obtained as a reaction product of an isocynate with a hydroxyl radical. The chemical composition of DB castor oil is approximately 90% triglyceride of Ricinoeic Acid of 928 molecular weight.

The procedure for the preparation of specimens involves vacuuming, heating, mixing and curing Solithane 113 and castor oil. As the Solithane 113 and the castor oil are hygroscopic materials, precautions are taken to minimize their contact with moisture in the air. To begin with, all

containers used in transferring and mixing the ingredients are dried in a desicator at least twelve hours before they are used. A predetermined amount of castor oil is transferred from the storage drum to the mixing and degassing container. After vacuuming the castor oil alone for two hours at 130°F, the proper amount of Solithane 113 (4 parts of castor oil to 3 parts of Solithane by weight) is added to the castor oil in the container. Using Pyromagnestir, the mixture is then heated at constant temperature of 130°F, vacuumed and thoroughly mixed. The mixture is then poured into molds which are previously sprayed with slipicone and flurog-lide assembled and preheated to 180°F. The mixture together with the molds is vacuumed again for twenty minutes in a large vacuum chamber. Finally, the cast molds are oven cured for two hours at 220°F. Upon removal from the oven, the specimens are released immediately, cleaned and stored in a desicator for two weeks for post curing.

Tubular specimens were used in the present investigations. A typical specimen with the various dimensions is shown in Fig. 2.

Experimental Arrangement

Two types of biaxial experiments were conducted. In the first type, the deformation rates were controlled and in the second, the axial stress rates were controlled. For the biaxial stress experiments with the controlled deformation rates, a standard Tinius Olsen was used [1]. The crosshead speed in the machine can be controlled between 0.02 in/min and 20 in/min.

---

* Number in brackets refer to the bibliography at the end.

The biaxial stress experiments with the controlled axial stress rates were conducted by using a specially developed apparatus that is described elsewhere [2].

The axial deformation and the variation of external diameter in the biaxial experiments were observed by using the clip gages.

Experimental Program and Procedure

(a) Deformation Rate Controlled Experiments

Tubular specimens were subjected to internal pressure by means of nitrogen gas fed from cylinders. The pressure is controlled by a valve which is placed in-between the outlet to the gas bottle and the inlet to the specimen. The axial load was applied by the loading mechanism of Tinius Olsen machine. The rate of deformation in a particular test was kept constant by setting the crosshead speed knob of the machine at a specified value on a circular dial. Biaxial stress experiments were conducted for crosshead speeds in ins/min, 0.2, 0.3, 0.4, 0.5, 1.0 and 2.0. Two experiments were conducted under identical conditions. During the test the pressure inside the specimen was measured by a pressure transdencer. The output from the pressure transducer was continuously recorded on the chart of a recorder. A continuous record of the axial load was obtained by the X-Y recorder of the Olsen Testing Machine. The external diameter and the axial displacement during a particular experiment were measured by clip gages. Continuous record of these quantities were obtained from a multi-channel Sanborn recorder. From the various measurements described earlier, true principal stresses σ_1, σ_2 and principal extension ratios λ_1 and λ_2 were evaluated as follows:

$$\sigma_1 = \frac{pD_m}{4t} + \frac{4F}{\pi(D_o^2 - D_i^2)} \qquad (1)$$

$$\sigma_2 = \frac{pD_m}{2t} \qquad (2)$$

where σ_1, σ_2, are the true axial and tangential stresses respectively.

Mean diameter

$$D_m = \frac{D_o + D_i}{2}$$

D_o, D_i are the outer and inner diameters respectively at any stage of deformation.

$t = \frac{D_o - D_i}{2}$ the wall thickness at any stage of deformation.

F = Axial Force

p = Internal Pressure

Assuming the material as incompressible, we have

$$\frac{\pi(D_o'^2 - D_i'^2)}{4} \ell' = \frac{\pi(D_o^2 - D_i^2)}{4} \ell \qquad (3)$$

where D_o', D_i' - original outer and inner diameters of the specimen respectively.

ℓ' - original gage length.

ℓ - gage length at any stage of deformation.

Equation (3) could be solved for D_i for known values of D_o, ℓ and the original dimensions of the specimen.

The expressions for extension ratios are:

$$\lambda_1 = \frac{\ell}{\ell'} \qquad (4)$$

$$\lambda_2 = \frac{D_m}{D_m'} \tag{5}$$

where λ_1 and λ_2 are the axial and tangential extension ratios respectively. Figs. 3 & 4 show the experimental results for various crosshead speeds and in Table 1, the various measured values are tabulated.

(b) Stress Rate Controlled Experiments

Tubular specimens were subjected to simultaneous internal pressure and axial load in such a manner that the principal nominal stresses varied linearly with time throughout the duration of the test. The biaxial experiments were conducted at various stress rates ranging from 0.1 to 10 psi. per second. The biaxial stress fields studied were $\alpha' = 0.383, 0.99,$ where $\alpha' = \frac{\sigma_2'}{\sigma_1'}$. the nominal principal stress ratio.

A continuous record of pressure, axial load for the duration of the test was obtained from a Sanborn recorder. The axial deformation and the variation in external diameter were determined from clip gages[3]. A continuous record of these quantities were also obtained through the Sanborn recorder.

From the various measured quantities true principal storage and extension ratios were evaluated by using Equations (1) to (5). The data are presented in Table 2 and Figs. 5 and 6.

Determination of Strain Energy Function

For an incompressible material the third stretch invariant I_3 being equal to one, the strain energy function becomes ~~only~~ a function only of the first two invariants. That is

$$W = W(I_1, I_2) \tag{6}$$

where

$$I_1 = \lambda_1^2 + \lambda_2^2 + \lambda_3^2$$

$$I_2 = \lambda_1^2 \lambda_2^2 + \lambda_2^2 \lambda_3^2 + \lambda_3^2 \lambda_1^2$$

$$I_3 = \lambda_1^2 \lambda_2^2 \lambda_3^2 = 1$$

Using the well-known finite deformation theory and the strain energy function expressed in terms of the two stretch invariants the constitutive equations for the rubberlike material can be shown to be

$$\sigma_1 = 2 \lambda_1^2 \left(\frac{\partial W}{\partial I_1} - \frac{1}{\lambda_1^2} \frac{\partial W}{\partial I_2} \right) - p$$

$$\sigma_2 = 2 \lambda_2^2 \left(\frac{\partial W}{\partial I_1} - \frac{1}{\lambda_2^2} \frac{\partial W}{\partial I_2} \right) - p$$

$$\sigma_3 = 2 \lambda_3^2 \left(\frac{\partial W}{\partial I_1} - \frac{1}{\lambda_3^2} \frac{\partial W}{\partial I_2} \right) - p \qquad (7)$$

Assuming $\sigma_3 = 0$, eliminating p - the unknown hydrostatic stress and solving for $\frac{\partial W}{\partial I_1}$ and $\frac{\partial W}{\partial I_2}$ we get

$$\frac{\partial W}{\partial I_1} = \frac{\dfrac{\lambda_1^2 \sigma_1}{\lambda_1^2 - 1/\lambda_1^2 \lambda_2^2} - \dfrac{\lambda_2^2 \sigma_2}{\lambda_2^2 - 1/\lambda_1^2 \lambda_2^2}}{2(\lambda_1^2 - \lambda_2^2)}$$

$$\frac{\partial W}{\partial I_2} = \frac{\dfrac{\sigma_1}{\lambda_1^2 - 1/\lambda_1^2\lambda_2^2} - \dfrac{\sigma_2}{\lambda_2^2 - 1/\lambda_1^2\lambda_2^2}}{2(\lambda_2^2 - \lambda_1^2)} \tag{8}$$

Substituting σ_1, σ_2, λ_1 and λ_2 in Equations (8) $\frac{\partial W}{\partial I_1}$ and $\frac{\partial W}{\partial I_2}$ can be evaluated.

The strain energy function can be explicitly determined if $\left(\frac{\partial W}{\partial I_1}\right)_{I_2 = \text{Constant}}$ and $\left(\frac{\partial W}{\partial I_2}\right)_{I_1 = \text{Constant}}$ are evaluated from Equations (8). That is possible if the appropriate values of λ_1, λ_2, σ_1, and σ_2 corresponding to either I_1 = Constant or I_2 = Constant are substituted in Equations (8).

It is generally difficult to conduct biaxial experiments with I_1 = Constant or I_2 = Constant. However, stress components corresponding a combination of λ_1 and λ_2 for which either I_1 or I_2 = Constant can be evaluated from the test data reported earlier.

The pairs of λ_1 and λ_2 representing I_1 = Constant or I_2 = Constant can be determined as follows:

The expression for the first stretch invariant is:

$$I_1 = \lambda_1^2 + \lambda_2^2 + \lambda_3^2 \tag{9}$$

Using the incompressibility condition $\lambda_3 = \frac{1}{\lambda_1\lambda_2}$ Equation (9) reduces to

$$\lambda_2^4 - (I_1 - \lambda_1^2)\lambda_2^2 + \frac{1}{\lambda_1^2} = 0 \tag{10}$$

Solving Equation (10):

$$\lambda_2^2 = \frac{1}{2}\left[(I_1 - \lambda_1^2) \pm \sqrt{(I_1 - \lambda_1^2)^2 - \frac{4}{\lambda_1^2}}\right] \tag{11}$$

The expression for the second stretch invariant is

$$I_2 = \lambda_1^2\lambda_2^2 + \frac{1}{\lambda_1^2} + \frac{1}{\lambda_2^2} \tag{12}$$

Rearranging Equation (12)

$$\lambda_1^2\lambda_2^4 - (I_2 - \frac{1}{\lambda_1^2})\lambda_2^2 + 1 = 0 \tag{13}$$

Solving Equation (13)

$$\lambda_2^2 = \frac{1}{2\lambda_1^2}\left[(I_2 - \frac{1}{\lambda_1^2}) \pm \sqrt{(I_2 - \frac{1}{\lambda_1^2})^2 - 4\lambda_1^2}\right] \tag{14}$$

Using Equation (11) for Constant I_1 and specified values of λ_1 values of λ_2 can be calculated. Similarly for constant values of I_2 λ_1 and λ_2 values can be evaluated by using Equation (14).

Figs. 7 to 10 show the λ_2 versus λ_1 curves obtained experimentally from two identical sets of biaxial stress experiments in which strain rates were controlled. In the same figures isoinvariant curves for which either I_1 or I_2 is constant have been drawn. The intersection of each of the curves with the λ_1 and λ_2 curves determines pairs of λ_1 and λ_2 with either I_1 or I_2 being constant. Using these values of λ_1 and λ_2 and the corresponding values of true stresses σ_1 and σ_2 obtained from Fig. 3, 4

the strain energy gradients $\frac{\partial W}{\partial I_2}$ and $\frac{\partial W}{\partial I_2}$ were evaluated by solving Equations (8). Figs. 11 to 21 show the variation of $\frac{\partial W}{\partial I_1}$ and $\frac{\partial W}{\partial I_2}$ with the true stress σ_1 for the various strain rates. Using the λ_1 versus time curves (See Figs. 22, 23) it is possible to determine the variation of $\frac{\partial W}{\partial I_1}$ and $\frac{\partial W}{\partial I_2}$ with time t. (See Figs. 24 to 27). The strain energy gradient values exponentially decrease with time reaching a constant value after the passage of about three to four minutes. The constant values corresponding to various I_1 or I_2 values were evaluated and plotted in Fig. 28. Fig. 28 indicates that $\frac{\partial W}{\partial I_1}$ is practically constant with I_1 although for small I_1 or I_2 there exists considerable oscillatory variation. Fig. 29 shows that $\frac{\partial W}{\partial I_2}$ is very small compared to $\frac{\partial W}{\partial I_1}$ and that it does remain invariant with I_2. In accordance with the above observations, the strain energy function for the material can be expressed by the following relation:

$$W = C(I_1 - 3) \tag{15}$$

where C = 15.5 (lbs./in.^{2}) represents the average value between two sets of results (Fig. 28).

The strain energy stored in the material at any stage of deformation was evaluated from the integration of the stress extension ratio curves and is shown plotted in Fig. 30. From Fig. 30 the "C" value was found to be 21.

By following the same procedure described earlier the results from the biaxial experiments with the controlled stress rates were used to

evaluate the strain energy function. The strain energy gradient value reached a steady state after a few minutes. These steady values were plotted in Figs. 31 and 32 against the strain invarients. As before, $\frac{\partial W}{\partial I_2}$ was found to be small enough to be neglected in comparison with $\frac{\partial W}{\partial I_1}$. Although $\frac{\partial W}{\partial I_1}$ showed some oscillatory variation for small values of I_1, it was fairly constant beyond I_1 value of 3.4. This constant value representing the constant C in Equation (15) was found to be 22. By direct integration of stress-extension ratio curves, an average value of C was evaluated to be 24.

Discussion of Results

Although Figs. 3 and 4 indicate that strain rate effects on the true stress extension ratio curves is small, the plots of tangential extension ratio against axial extension ratio (Figs. 7 to 10) show appreciable effects due to strain rate. True tangential stress was practically held constant during all the strain rate controlled experiments.

The strain energy gradient plots against invariants showed oscillatory variation for low values of invariants. This behavior may be due to experimental errors which are extremely difficult to eliminate at low extension ratios.

It is interesting to note that the equilibrium mechanical behavior of Solithane 113 can be described by a simple strain energy function of Neo Hookean type (Equation 15).

Bibliography

1. M. G. Sharma and C. K. Lim, "Mechanical Properties of Solid Fuel Propellants for Combined States of Stress at Various Temperatures", Annual Report submitted to the Allegany Ballistics Laboratory (NORD 16640-Sub-contract 70), Sept. 1963.
2. M. G. Sharma and C. K. Lim, "Failure Criteria for Viscoelastic Materials under Biaxial Stress Fields", Tech. Report No. 4, NASA-JPL Contract No. 950875, Sept. 1967.
3. M. G. Sharma and C. K. Lim, "Failure of an Inert Composite Propellant under Multi-axial Stress Fields", Technical Report No. 1, NASA-JPL Contract No. 950875, March 1965.

Table 1
Biaxial Stress-strain Data for Solithane 113
(Strain rate controlled experiments)

Experiment No.	Axial Rate of Displacement	Time (Min.)	True Axial Stress σ_{11} (p.s.i.)	True Tangential Stress σ_{22} (p.s.i.)	Axial Extension Ratio λ_1 (in./in.)	Tangential Extension Ratio λ_2 (in./in)	$\frac{\partial W}{\partial I_1}$ (p.s.i.)	$\frac{\partial W}{\partial I_2}$ (p.s.i.)
I	0.2 (in./min.)	0.5000	1.66854	0.78288	1.0080	1.0081	0706.59	79438.703
		1.5000	5.72268	3.83796	1.040	1.0295	182.38	- 159.169
		2.5000	10.94164	10.50197	1.066	1.0575	4.034	10.390
		3.5000	14.93735	12.77806	1.088	1.0509	4.054	12.477
		4.5000	17.61665	12.36876	1.100	1.0362	17.379	2.445
		5.5000	19.76648	11.67095	1.116	1.0309	27.013	- 6.437
		6.5000	22.38613	11.78038	1.136	1.0184	19.084	1.670
		7.5000	24.69378	11.45322	1.152	1.0081	21.853	- 0.755
		8.5000	26.67390	10.8649	1.214	0.9999	16.488	0.287
		9.5000	28.61544	10.66180	1.226	0.9918	17.785	0.0645
		10.5000	30.49202	10.46951	1.244	0.9864	17.512	- 0.542
		11.5000	32.05114	11.00261	1.268	0.9857	16.512	0.0489
		12.5000	32.82635	10.73434	1.268	0.9714	15.086	2.346
II	0.2	7.000	3.32477	2.19675	1.0080	1.0067	4346.116	- 4251.880
		2.000	7.34779	5.35053	1.0400	1.0188	45.001	- 24.812
		3.000	11.79961	10.11073	1.0600	1.0376	11.549	7.732
		4.000	15.28858	12.77806	1.0840	1.0509	15.107	3.436
		5.000	17.72092	12.12138	1.1160	1.0362	12.876	4.589
		6.000	20.26614	11.86812	1.1480	1.0269	13.794	2.980
		7.000	22.23507	11.42697	1.1800	1.0148	12.610	3.289
		8.000	24.54437	11.27281	1.2040	1.0067	13.689	2.240
		9.000	26.47835	10.75218	1.2320	0.9932	13.163	2.447
		10.000	28.33652	10.36362	1.2520	0.9844	13.807	1.833
		11.000	30.22384	9.72468	1.2760	0.9714	13.889	1.667
		12.000	32.15223	9.49425	1.2960	0.9639	14.251	1.317
		13.000	33.86162	9.25387	1.3120	0.9536	14.000	1.800
		14.000	35.80580	9.06270	1.3340	0.9454	13.995	1.748
		15.000	37.50195	8.80935	1.3500	0.9343	13.573	2.446
		16.000	39.33546	9.14817	1.372	0.927	13.826	1.850
		17.000	41.14488	8.96836	1.388	0.919	13.887	1.949
		18.000	42.74406	8.78941	1.408	0.915	13.687	2.063
		19.000	44.39072	8.70835	1.418	0.916	14.135	1.820
		20.000	45.98131	8.49052	1.430	0.912	14.658	1.350
I	0.3	0.25	1.11109	0.62992	1.006	1.003	772.808	- 749.765
		1.25	6.30599	2.59168	1.064	1.015	51.364	- 38.178
		2.25	13.85383	10.97525	1.080	1.035	3.709	14.213
		3.25	18.38158	12.55648	1.112	1.026	5.156	13.787
		4.25	22.08996	12.25452	1.144	1.011	10.114	9.378
		5.25	25.17257	11.64819	1.172	0.993	10.524	9.407
		6.25	28.30811	11.16411	1.204	0.976	9.812	10.212
		7.25	31.43908	10.65535	1.254	0.960	10.636	7.764

Table 1
Biaxial Stress-strain Data for Solithane 113
(Strain rate controlled experiments)

Experiment No.	Axial Rate of Displacement	Time (Min.)	True Axial Stress σ_{11} (p.s.i.)	True Tangential Stress σ_{22} (p.s.i.)	Axial Extension Ratio λ_1 (in./in.)	Tangential Extension Ratio λ_2 (in./in)	$\frac{\partial W}{\partial I_1}$ (p.s.i.)	$\frac{\partial W}{\partial I_2}$ (p.s.i.)
II	0.3 (in./min.)	1.00	5.27952	2.50374	1.032	0.9999	27.012	6.063
		2.00	10.32089	5.26839	1.068	1.0027	15.122	4.071
		3.00	15.11131	8.89419	1.110	1.0150	9.974	6.840
		4.00	19.62281	12.36568	1.144	1.0188	4.301	12.364
		5.00	22.08943	11.44623	1.196	1.0067	8.181	6.643
		6.00	25.03536	11.30835	1.208	0.9973	11.421	4.858
		7.00	27.72823	10.91033	1.216	0.9864	13.974	3.822
		8.00	30.36047	11.02211	1.244	0.9783	13.906	3.654
		9.00	32.62590	10.29394	1.276	0.9625	13.430	3.745
		10.00	35.11222	10.23534	1.306	0.9522	13.067	3.871
		11.00	37.47452	10.54147	1.380	0.9412	11.797	2.809
		12.00	39.94010	9.93532	1.420	0.9329	11.733	2.381
		13.00	41.96548	9.78031	1.452	0.9232	11.475	2.403
		14.00	44.35607	9.49477	1.484	0.9120	11.433	2.352
		15.00	46.43077	9.28191	1.516	0.9040	11.376	2.17
I	0.4	0.95	6.65387	4.72674	1.046	1.011	- 10.571	26.672
		1.95	15.51593	11.41694	1.096	1.033	6.597	11.093
		2.95	20.66554	10.90230	1.152	1.008	10.450	7.081
		3.95	24.93499	11.08818	1.200	0.993	11.090	5.930
		4.95	28.71683	10.14980	1.246	0.971	11.964	4.812
		5.95	31.48122	9.76082	1.280	0.958	12.107	4.437
		6.95	35.01626	9.22954	1.330	0.936	11.180	5.035
		7.95	38.57375	8.57012	1.440	0.915	10.541	2.783
II	0.4	0.25	1.97842	0.68718	1.016	1.003	244.995	- 229.361
		1.25	6.44897	4.24094	1.044	1.015	32.177	- 15.511
		2.25	11.66899	10.29682	1.068	1.038	- 11.597	27.385
		3.25	15.68598	12.61613	1.096	1.036	- 4.506	21.346
		4.25	18.26993	11.98171	1.120	1.022	5.298	12.721
		5.25	20.9730	11.61262	1.154	1.011	8.729	8.659
		6.25	23.51767	11.68208	1.178	1.002	10.384	7.105
		7.25	25.81090	11.18509	1.204	0.988	10.571	6.944
		8.25	28.14451	10.77034	1.248	0.977	10.808	5.342
		9.25	30.20092	10.52168	1.288	0.967	10.787	4.375
		9.35	30.47862	10.36350	1.360	0.963	9.022	3.241
I	0.5	0.50	6.60113	7.58291	1.024	1.004	- 688.496	714.945
		1.00	10.81069	8.66648	1.060	1.024	- 7.992	26.347
		1.50	15.74491	12.27628	1.088	1.033	- 0.280	19.092
		2.00	19.04029	12.14282	1.120	1.022	7.980	10.956
		2.50	21.74700	11.46422	1.160	1.007	9.876	7.739
		3.00	24.37870	11.71905	1.188	1.004	12.215	4.951
					1.216	0.993	11.707	4.923

Table 1
Biaxial Stress-strain Data for Solithane 113
(Strain rate controlled experiments)

Experiment No.	Axial Rate of Displacement	Time (Min.)	True Axial Stress σ_{11} (p.s.i.)	True Tangential Stress σ_{22} (p.s.i.)	Axial Extension Ratio λ_1 (in./in.)	Tangential Extension Ratio λ_2 (in./in.)	$\frac{\partial W}{\partial I_1}$ (p.s.i.)	$\frac{\partial W}{\partial I_2}$ (p.s.i.)
I	0.5 (in./min.)	4.00	29.14935	11.13138	1.240	0.982	13.087	3.927
		4.50	31.20176	11.19919	1.272	0.975	12.501	3.811
		5.00	33.38915	10.46208	1.312	0.957	11.704	3.989
		5.25	34.32029	10.35457	1.320	0.953	11.862	3.956
II	0.5	0.50	5.13514	2.49578	1.024	0.999	- 24.295	52.275
		1.00	9.22307	3.82862	1.064	1.015	74.011	- 55.547
		1.50	16.24720	13.27834	1.096	1.034	- 10.664	28.007
		2.00	19.65488	12.44615	1.120	1.017	5.293	14.486
		2.50	22.63862	11.60823	1.154	0.999	7.969	11.522
		3.00	25.42877	11.42419	1.188	0.993	11.482	6.958
		3.50	28.38985	11.34629	1.212	0.978	10.587	8.517
		4.00	31.31795	11.34430	1.240	0.967	10.572	8.598
		4.50	34.12913	11.05851	1.268	0.956	11.566	7.464
		5.00	36.45584	10.64273	1.296	0.941	10.503	8.566
		5.50	38.87541	10.41762	1.324	0.933	11.265	7.406
		6.00	41.23407	10.39158	1.360	0.923	11.080	6.906
		6.50	43.20571	9.78614	1.384	0.909	10.552	7.591
		7.00	45.59251	9.49217	1.412	0.898	10.406	7.707
		7.40	47.24292	9.27301	1.432	0.889	10.142	7.999
I	1.0	0.1	2.57122	2.89955	1.012	1.008	- 731.873	740.215
		0.2	4.22740	3.65343	1.024	1.008	- 116.055	133.101
		0.3	6.43166	5.19358	1.028	1.011	- 50.664	73.705
		0.4	8.78124	7.88256	1.048	1.017	- 65.919	83.056
		0.5	11.50820	11.10766	1.072	1.026	- 56.330	70.564
		1.00	18.77436	12.36940	1.130	1.015	- 1.774	19.374
		1.50	24.27051	11.49771	1.192	0.996	9.414	7.711
		2.00	29.84291	11.11315	1.252	0.982	13.379	3.217
		2.50	34.50410	10.73211	1.300	0.967	14.605	1.824
		3.00	39.40960	10.75133	1.364	0.956	14.553	1.014
		3.50	43.43974	10.35737	1.416	0.945	14.673	0.377
		4.00	47.57415	9.87422	1.472	0.93428	14.640	- 0.136
		4.50	51.58053	9.76240	1.536	0.92246	13.870	- 0.015
		4.58	51.95239	9.48698	1.716	0.91897	10.013	0.241
II	1.0	0.25	5.83135	4.61748	1.048	1.006	- 53.986	67.838
		0.50	12.99883	14.53329	1.080	1.036	- 83.525	94.237
		0.75	16.52295	15.21357	1.116	1.036	- 25.515	39.221
		1.00	19.57263	14.98633	1.144	1.030	- 6.577	21.911
		1.25	22.75230	14.73750	1.168	1.022	3.106	13.458
		1.50	25.58140	14.48987	1.188	1.015	8.195	9.214
		1.75	28.34090	14.24342	1.200	1.007	12.079	6.574
		2.00	30.79353	13.77055	1.289	0.9999	10.390	4.189
		2.02	31.98772	13.77055	1.336	0.9999	9.747	3.313

Table 1
Biaxial Stress-strain Data for Solithane 113
(Strain rate controlled experiments)

Experiment No.	Axial Rate of Displacement	Time (Min.)	True Axial Stress σ_{11} (p.s.i.)	True Tangential Stress σ_{22} (p.s.i.)	Axial Extension Ratio λ_1 (in./in.)	Tangential Extension Ratio λ_2 (in./in)	$\frac{\partial W}{\partial I_1}$ (p.s.i.)	$\frac{\partial W}{\partial I_2}$ (p.s.i.)
I	2.0 (in./min.)	0.25	7.92948	2.46404	1.06	0.993	41.493	- 23.907
		0.50	18.96297	13.61414	1.12	1.019	- 7.940	26.430
		0.75	25.88744	15.21963	1.178	1.012	5.387	13.210
		1.00	31.27360	13.77623	1.228	0.993	12.633	6.161
		1.25	36.47280	13.66375	1.288	0.983	14.369	3.362
		1.50	41.55897	14.58809	1.336	0.978	14.656	2.788
		1.75	45.80130	13.56322	1.384	0.964	15.460	1.569
		2.00	50.24459	13.31117	1.442	0.956	15.428	0.812
		2.25	54.63334	12.94671	1.496	0.945	15.235	0.539
		2.30	55.19947	12.81069	1.504	0.941	15.074	0.657
II	2.0	0.25	10.28386	7.96104	1.066	1.012	- 32.141	49.481
		0.50	19.56638	15.30541	1.124	1.028	- 10.719	28.119
		0.75	25.38622	14.86841	1.184	1.012	5.305	12.386
		1.00	31.08862	14.79481	1.236	0.999	10.947	6.858
		1.25	35.98603	14.46670	1.290	0.990	13.498	3.684
		1.33	37.48578	14.85618	1.300	0.990	13.910	3.40

Table 2
Biaxial Stress-strain Data for Solithane 113
(Stress rate controlled experiments)

Test No.	Nominal Stress Ratio	Time (Sec.)	True Axial Stress σ_{11} (p.s.i.)	True Tangential Stress σ_{22} (p.s.i.)	Axial Extension Ratio λ_1 (in./in.)	Tangential Extension Ratio λ_2 (in./in)	$\frac{\partial W}{\partial I_1}$ (p.s.i.)	$\frac{\partial W}{\partial I_2}$ (p.s.i.)
I	0.383	0.00	0.000	-0.000	1.000	1.000	0000.0000	0000.0000
		1.00	8.227	2.761	1.052	0.989	0.6207	22.4758
		2.00	13.414	4.882	1.081	0.985	4.3006	19.5493
		3.00	20.605	7.764	1.129	0.987	18.1325	4.0395
		4.00	29.789	11.573	1.182	0.992	21.6602	0.6132
		5.00	41.472	16.828	1.251	1.002	21.1968	1.1315
		6.00	61.907	26.133	1.369	1.032	21.6586	0.8161
		7.00	85.627	39.091	1.490	1.091	22.2472	0.8238
		8.00	114.672	60.487	1.629	1.211	22.5505	0.9292
		9.00	144.295	92.188	1.753	1.388	22.5134	1.2014
II	0.383	0.00	0.000	-0.000	1.000	1.000	0000.0000	0000.0000
		10.00	4.565	1.640	1.026	0.993	-141.5349	169.8239
		20.00	7.276	2.687	1.045	0.994	21.6148	0.4640
		30.00	11.137	4.276	1.068	0.991	12.1539	10.5228
		40.00	16.521	6.400	1.103	0.991	21.2818	0.5042
		50.00	24.933	9.775	1.154	0.993	21.9657	-0.1058
		60.00	35.330	14.249	1.218	0.997	20.7693	1.1480
		70.00	46.690	19.550	1.283	1.011	21.1485	1.0631
		80.00	64.219	28.763	1.381	1.046	21.2385	1.1205
III	0.383	0.00	0.000	-0.000	1.000	1.000	0000.0000	0000.0000
		10.00	4.241	1.484	1.026	0.995	7.1207	15.9658
		20.00	7.204	2.519	1.045	0.994	32.4518	-10.7269
		30.00	10.563	3.847	1.064	0.992	26.4253	-4.1090
		40.00	15.001	5.725	1.092	0.992	23.8723	-1.9890
		50.00	22.553	8.803	1.141	0.992	21.7943	-0.2218
		60.00	32.325	12.834	1.199	0.995	21.2671	0.7220
		70.00	41.589	17.085	1.257	1.006	21.6409	0.2913
		80.00	55.683	23.853	1.334	1.026	21.3856	0.9291
		90.00	76.159	36.079	1.440	1.080	21.5453	1.1790
		98.00	101.232	54.506	1.561	1.182	22.1560	1.0419
IV	0.383	0.00	0.000	-0.000	1.000	1.000	0000.0000	0000.0000
		10.00	5.217	1.663	1.035	0.995	45.3863	-24.9743
		20.00	9.433	3.406	1.058	0.994	32.2746	-10.3416
		30.00	14.134	5.266	1.090	0.992	24.5342	-3.3022
		40.00	20.392	7.804	1.128	0.994	25.0135	-3.7398
		50.00	29.934	11.731	1.185	0.997	23.1487	-1.3745
		60.00	42.353	17.256	1.257	1.005	21.6877	0.5337
		70.00	59.689	25.399	1.357	1.030	21.5006	0.8934
		80.00	86.295	41.397	1.488	1.103	22.1089	1.0713
		90.00	122.562	75.484	1.646	1.297	22.6593	1.1621
		92.00	130.043	85.051	1.672	1.347	22.7119	1.2804

Table 2
Biaxial Stress-strain Data for Solithane 113
(Stress rate controlled experiments)

Test No.	Nominal Stress Ratio	Time (Sec.)	True Axial Stress σ_{11} (p.s.i.)	True Tangential Stress σ_{22} (p.s.i.)	Axial Extension Ratio λ_1 (in./in)	Tangential Extension Ratio λ_2 (in./in.)	$\frac{\partial W}{\partial I_1}$ (p.s.i.)	$\frac{\partial W}{\partial I_2}$ (p.s.i.)
V	0.383	0.00	0.000	-0.000	1.000	1.000	0000.0000	0000.0000
		40.00	4.589	1.658	1.030	0.996	31.5159	-10.5082
		80.00	6.655	2.341	1.039	0.995	42.6380	-19.4370
		120.00	9.412	3.402	1.055	0.994	37.4291	-14.6670
		160.00	12.208	4.566	1.073	0.992	22.0814	0.6525
		200.00	16.892	6.612	1.103	0.994	24.7819	-2.7710
		240.00	25.083	9.895	1.154	0.994	22.5490	-0.6294
		280.00	35.017	14.140	1.216	0.998	21.1353	0.7824
		320.00	49.591	20.665	1.301	1.014	21.2562	0.9364
		360.00	70.679	31.620	1.411	1.055	21.7529	1.9828
		388.00	90.984	45.382	1.510	1.127	22.2115	1.0330
VI	0.383	0.00	-0.000	-0.000	1.000	1.000	0000.0000	0000.0000
		40.00	8.623	2.680	1.050	0.990	26.1718	-2.0450
		80.00	11.597	4.099	1.068	0.990	22.4939	1.0598
		120.00	16.242	5.836	1.093	0.987	19.3040	5.0067
		160.00	22.461	8.289	1.127	0.986	21.3057	3.1318
		200.00	28.639	10.865	1.165	0.990	23.3185	0.2641
		240.00	35.243	13.810	1.202	0.993	22.5704	1.1054
		280.00	46.700	18.719	1.266	1.003	22.9803	0.7818
		320.00	65.303	27.953	1.362	1.034	23.3718	0.7555
		360.00	88.293	41.939	1.473	1.100	23.9374	0.6223
		380.00	103.893	54.885	1.541	1.169	24.0872	0.7782
VII	0.383	0.00	-0.000	-0.000	1.000	1.000	0000.0000	0000.0000
		300.00	8.884	2.752	1.052	0.988	-0.8114	26.2202
		600.00	17.841	6.324	1.111	0.983	14.0615	8.8412
		900.00	29.539	11.221	1.177	0.992	23.0505	-0.4131
		1200.00	45.071	18.025	1.266	1.005	22.6030	0.2934
		1410.00	66.823	28.692	1.384	1.040	22.4440	0.8100
VIII	0.383	0.00	0.000	-0.000	1.000	1.000	0000.0000	0000.0000
		300.00	7.767	2.678	1.054	0.988	-8.6301	29.8226
		600.00	11.716	4.241	1.074	0.984	-8.0119	31.4821
		900.00	16.307	5.729	1.102	0.988	24.2650	-2.2665
		1200.00	21.048	7.979	1.135	0.990	21.4496	-0.3319
		1800.00	36.173	14.483	1.227	0.998	20.5242	1.0158
		2160.00	80.742	39.083	1.474	1.099	21.1473	1.1511
		2190.00	85.098	42.655	1.489	1.122	21.8598	0.8246
IX	0.383	0.00	-0.000	-0.000	1.000	1.000	0000.0000	0000.0000
		600.00	7.620	2.482	1.044	0.988	-50.0046	77.1150
		1320.00	10.410	3.601	1.059	0.986	-20.3352	47.0496
		1980.00	13.239	4.661	1.074	0.984	-6.1640	32.8529
		2400.00	14.452	5.150	1.083	0.986	9.6919	15.3179
		3000.00	16.261	5.884	1.093	0.984	9.8335	15.2038

Table 2
Biaxial Stress-strain Data for Solithane 113
(Stress rate controlled experiments)

Test No.	Nominal Stress Ratio	Time (Sec.)	True Axial Stress σ_{11} (p.s.i.)	True Tangential Stress σ_{22} (p.s.i.)	Axial Extension Ratio λ_1 (in./in.)	Tangential Extension Ratio λ_2 (in./in)	$\frac{\partial W}{\partial I_1}$ (p.s.i.)	$\frac{\partial W}{\partial I_2}$ (p.s.i.)
IX	0.383	3600.00	18.841	7.027	1.111	0.983	9.8977	14.4644
		4200.00	21.047	8.028	1.120	0.985	15.7594	8.8500
		4800.00	23.449	9.118	1.136	0.988	18.8246	4.9478
		6000.00	27.886	10.952	1.163	0.991	21.7283	1.6102
		7200.00	36.991	14.877	1.213	0.997	22.6088	0.8958
		8400.00	49.134	20.221	1.279	1.010	23.1193	0.5548
		9180.00	57.855	23.956	1.318	1.020	24.3213	0.1275
I	0.99	0.00	0.000	-0.000	1.000	1.000	7578.7260	87578.2020
		10.00	0.673	-0.000	1.004	1.001	3184.0733	-3159.6812
		20.00	0.915	0.570	1.004	1.001	4.8472	22.4872
		30.00	2.008	1.739	1.008	1.006	456.4472	-427.6376
		40.00	4.678	4.544	1.018	1.016	-47.1600	68.0292
		50.00	10.013	10.647	1.039	1.044	56.6706	-31.8066
		60.00	18.596	20.795	1.071	1.092	26.4862	-3.3962
		70.00	27.687	32.794	1.105	1.151	26.0062	-2.3356
		80.00	41.101	52.428	1.157	1.251	25.4893	-1.0205
		90.00	61.891	86.560	1.240	1.422	25.5265	-0.0416
		100.00	98.419	152.355	1.396	1.715	27.1100	0.2198
II	0.99	0.00	0.000	-0.000	1.000	1.000	7578.7260	87578.2020
		40.00	3.079	2.617	1.017	1.010	-0.1428	17.8654
		80.00	4.839	4.500	1.021	1.019	254.0417	-224.7483
		120.00	7.213	7.460	1.035	1.034	-460.6359	448.1710
		160.00	10.429	10.875	1.046	1.049	75.2459	-49.5540
		200.00	13.573	14.783	1.059	1.067	65.2523	-39.7071
		240.00	18.384	20.615	1.074	1.096	28.6666	-6.1989
		280.00	23.072	26.592	1.096	1.127	31.2298	-7.9739
		320.00	28.645	34.067	1.117	1.167	24.9772	-2.3792
		360.00	33.500	41.597	1.137	1.207	26.3991	-3.0557
		400.00	41.402	53.003	1.167	1.269	23.4505	-0.3718
III	0.99	0.00	0.000	-0.000	1.000	1.000	7578.7260	87578.2020
		60.00	4.332	4.121	1.021	1.015	-83.2562	99.8826
		120.00	7.799	8.045	1.032	1.032	2395.9971	-2228.7872
		180.00	12.179	13.218	1.049	1.057	57.5191	-32.4330
		240.00	19.119	21.853	1.074	1.099	30.8655	-7.4645
		300.00	27.019	32.094	1.107	1.152	27.4468	-3.9610
		360.00	34.877	43.624	1.135	1.212	24.6512	-1.1517
		420.00	43.565	54.955	1.172	1.270	24.0013	-0.2371
		480.00	42.320	52.837	1.164	1.258	22.9180	0.5458
		540.00	44.174	57.201	1.167	1.286	21.7770	1.3908
		600.00	45.378	59.262	1.168	1.295	21.3461	1.8471
		660.00	69.260	96.511	1.267	1.492	21.4023	2.1216
		670.00	76.061	107.392	1.295	1.546	21.4326	2.1691

Table 2
Biaxial Stress-strain Data for Solithane 113
(Stress rate controlled experiments)

Test No.	Nominal Stress Ratio	Time (Sec.)	True Axial Stress σ_{11} (p.s.i.)	True Tangential Stress σ_{22} (p.s.i.)	Axial Extension Ratio λ_1 (in./in.)	Tangential Extension Ratio λ_2 (in./in.)	$\frac{\partial W}{\partial I_1}$ (p.s.i.)	$\frac{\partial W}{\partial I_2}$ (p.s.i.)
IV	0.99	0.00	0.000	-0.000	1.000	1.000	7578.7260	87578.2020
		20.00	2.152	2.076	1.008	1.007	381.4187	-352.2782
		40.00	3.269	2.686	1.013	1.009	299.2809	-270.5078
		60.00	3.636	3.503	1.019	1.014	-113.6875	127.8619
		80.00	4.597	4.342	1.019	1.021	-498.4371	497.3981
		100.00	5.975	5.952	1.019	1.024	-179.6214	194.5925
		120.00	7.485	7.528	1.031	1.034	-77.9898	92.0098
		140.00	9.085	9.349	1.036	1.041	-20.2563	38.3480
		160.00	10.759	11.463	1.044	1.051	24.9156	-3.7265
		180.00	12.051	12.741	1.048	1.058	2.1239	17.1568
		200.00	13.871	15.115	1.055	1.070	15.9221	4.4761
		220.00	16.334	18.062	1.064	1.085	15.2334	5.1783
		240.00	18.759	21.260	1.073	1.101	19.0793	2.0139
		251.00	19.952	22.627	1.077	1.105	21.6279	0.2743

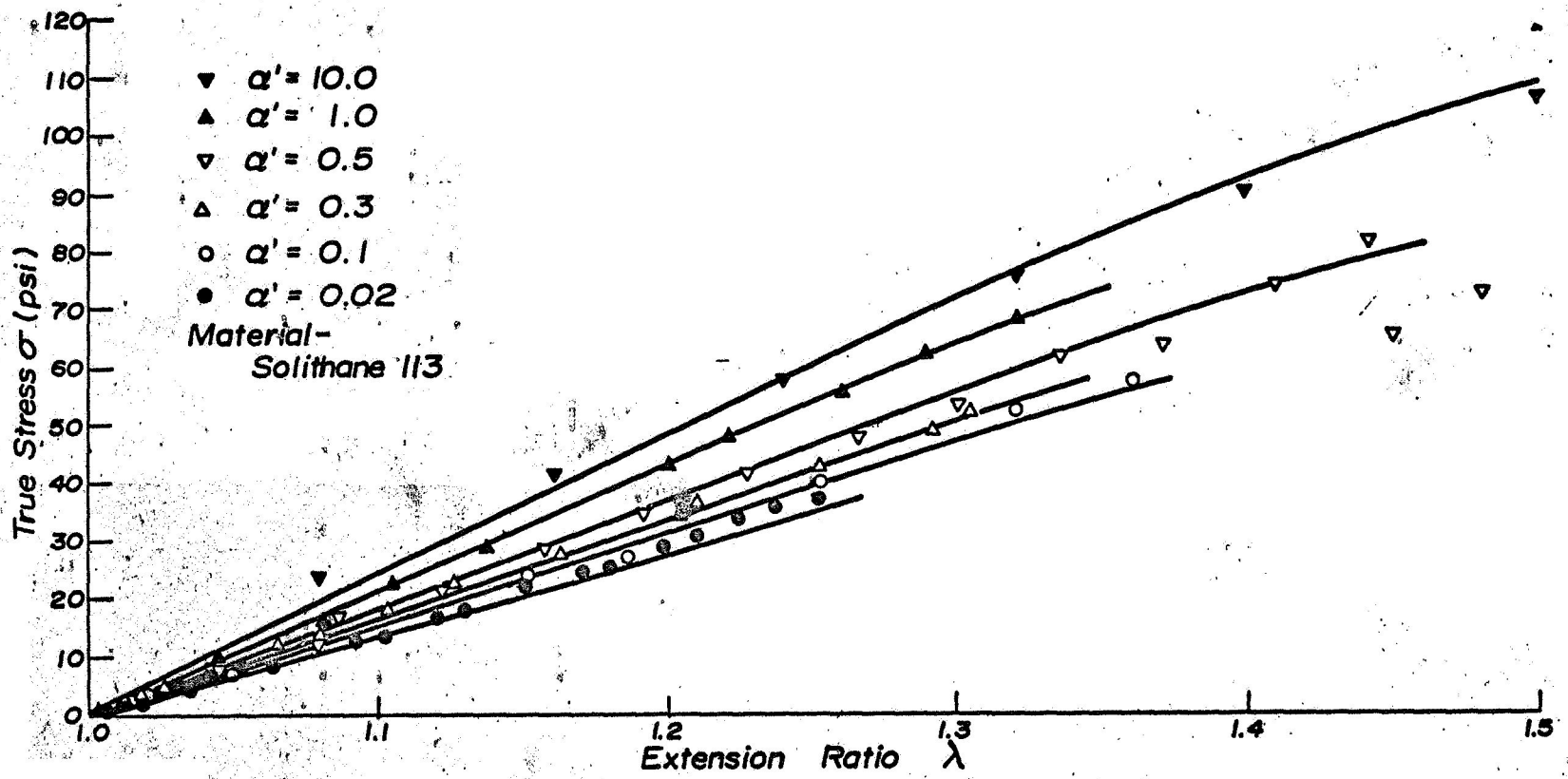

Figure 1. True Stress Versus Extension Ratio Curves in Tension for Solithane 113.

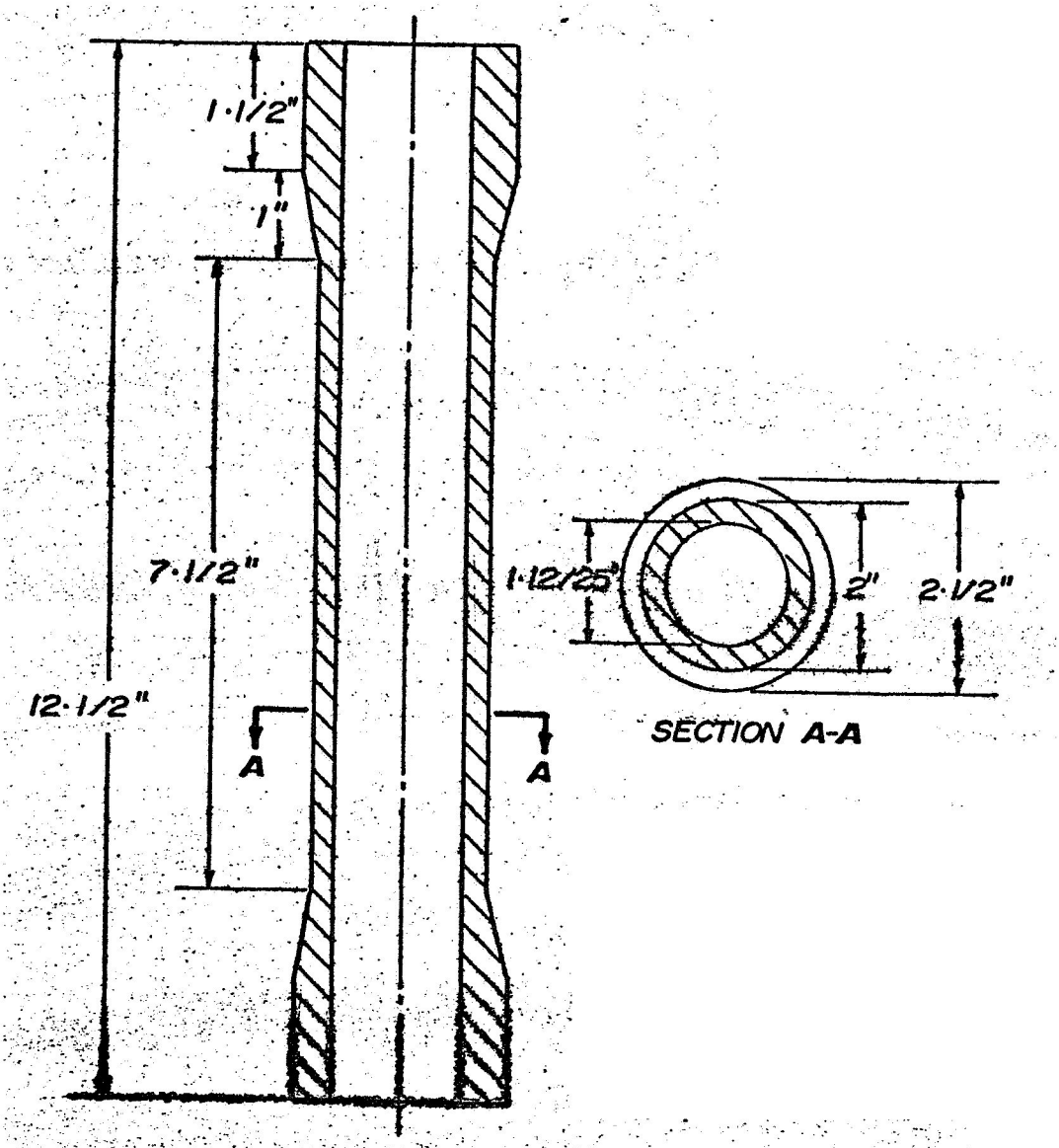

Figure 2. Typical Specimen of Solithane 113

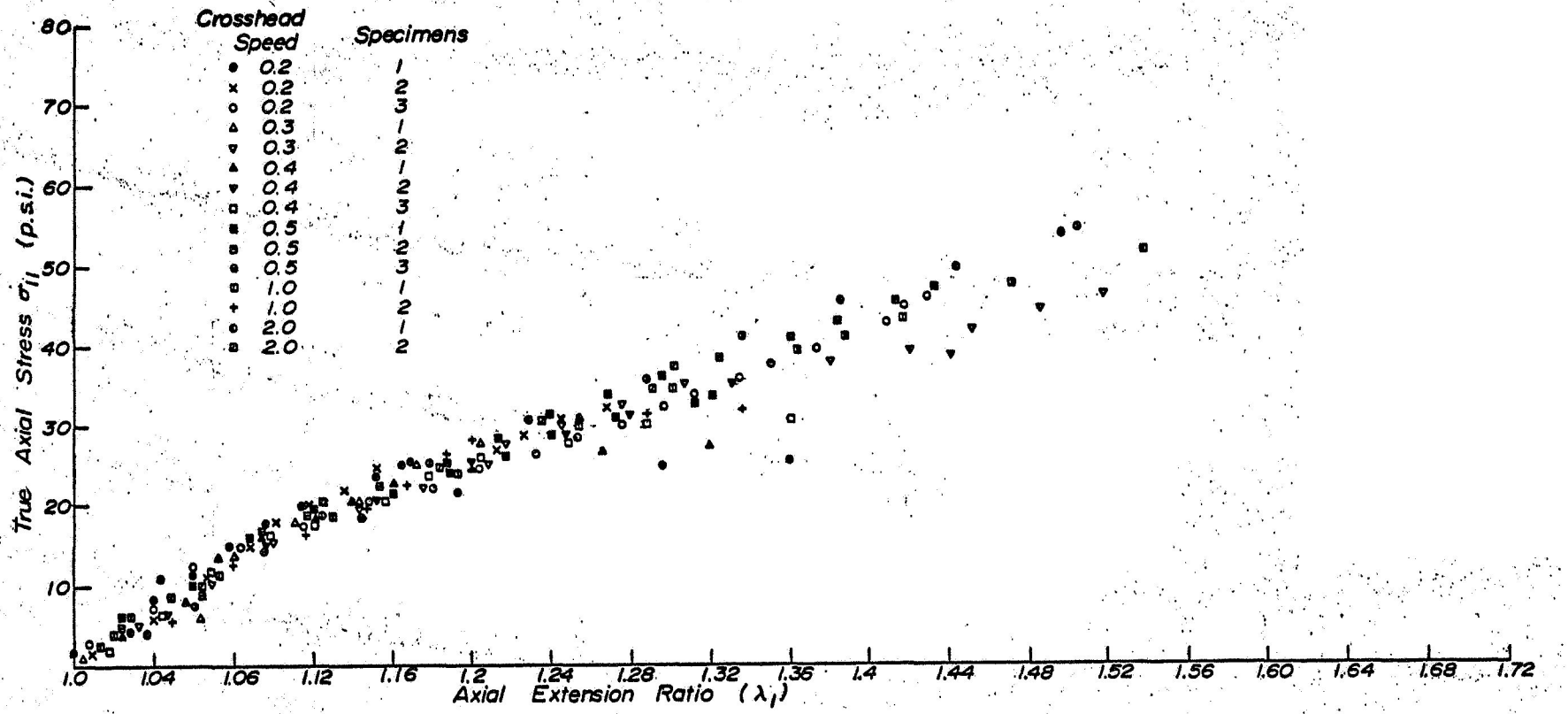

Figure 3. True Axial Stress Versus Axial Extension Ratio for Various Crosshead Speeds.

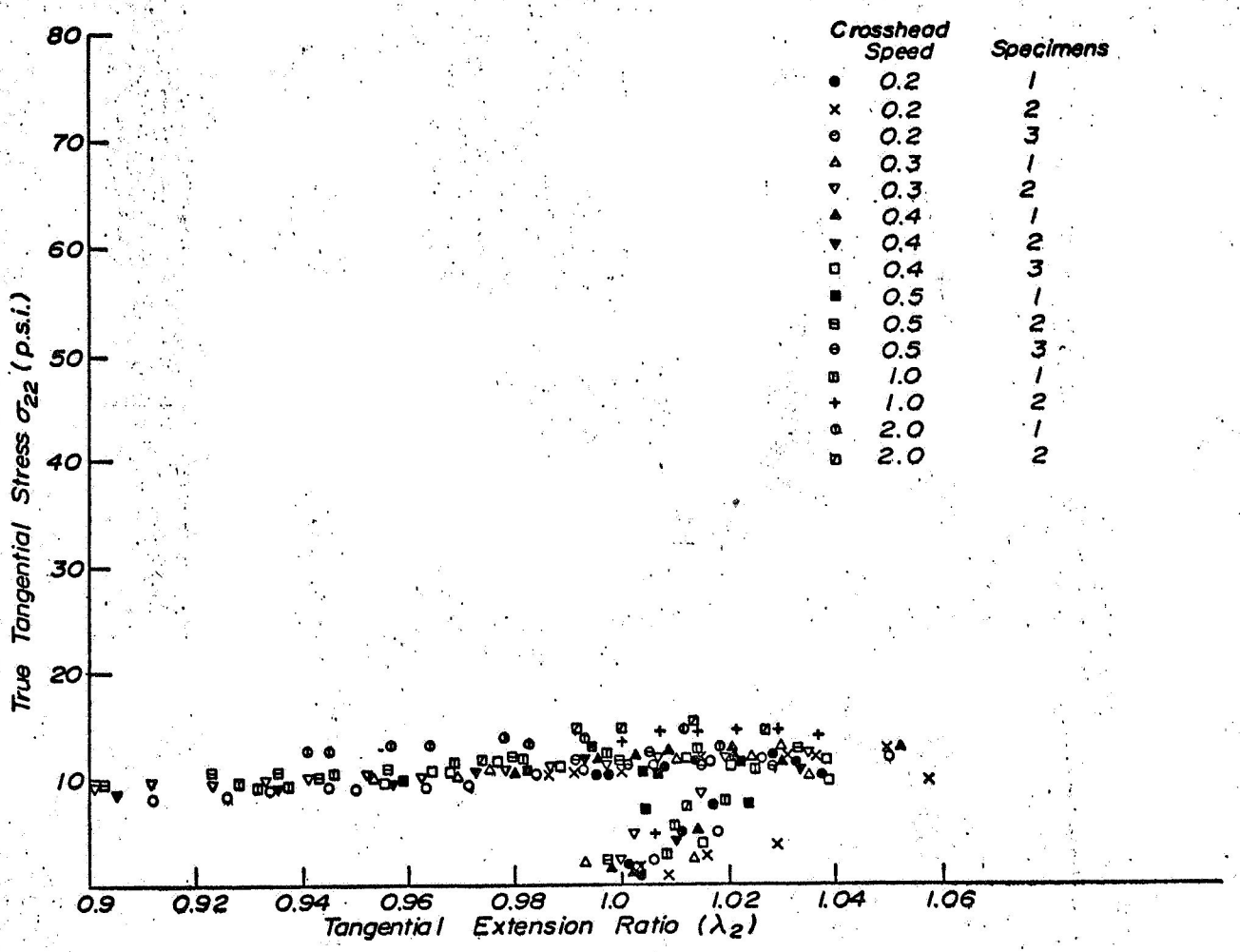

Figure 4. True Tangential Stress Versus Tangential Extension Ratio for Various Crosshead Speeds.

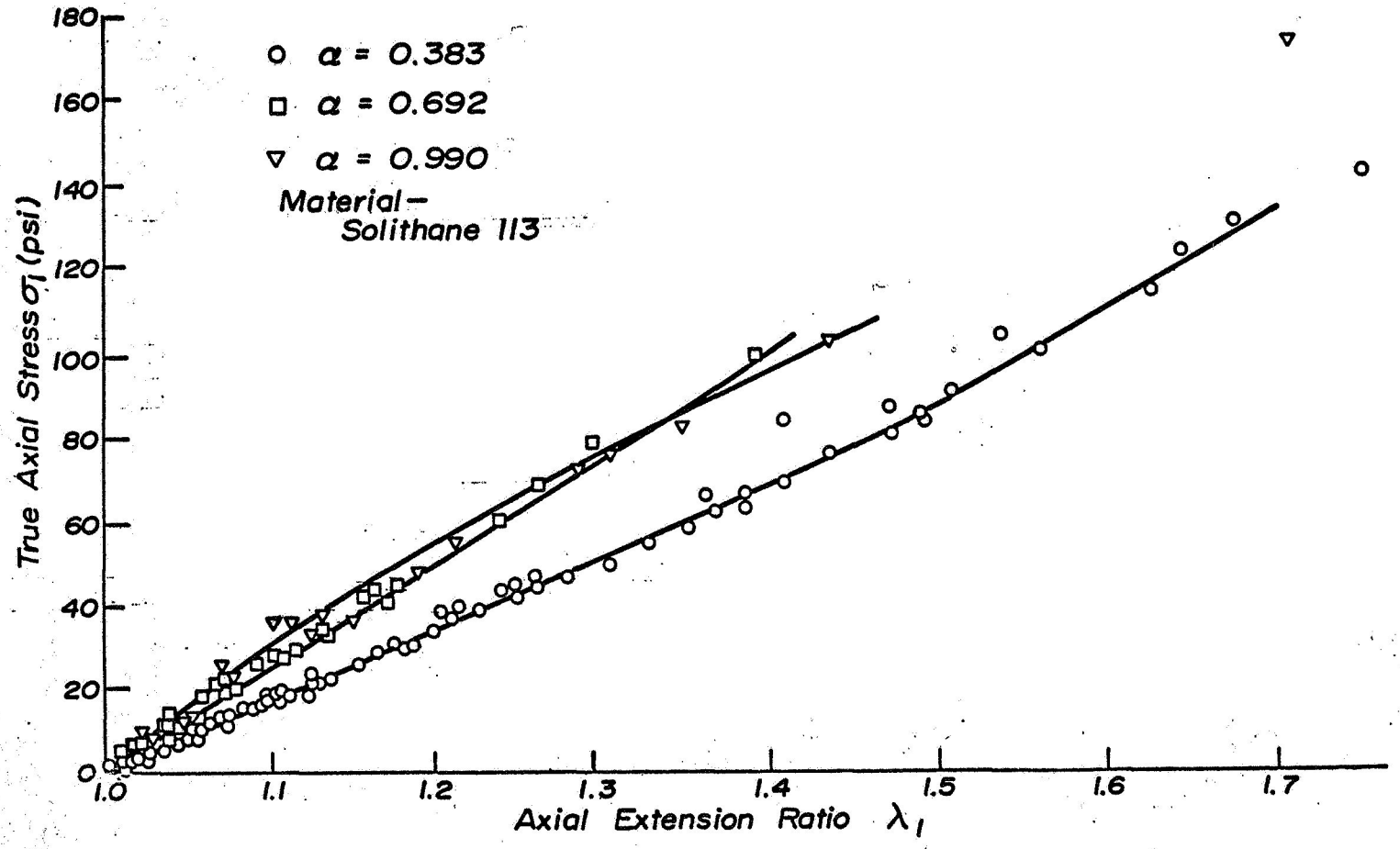

Figure 5. True Axial Stress Versus Axial Extension Ratio Curves for Solithane 113 Under Biaxial Loading.

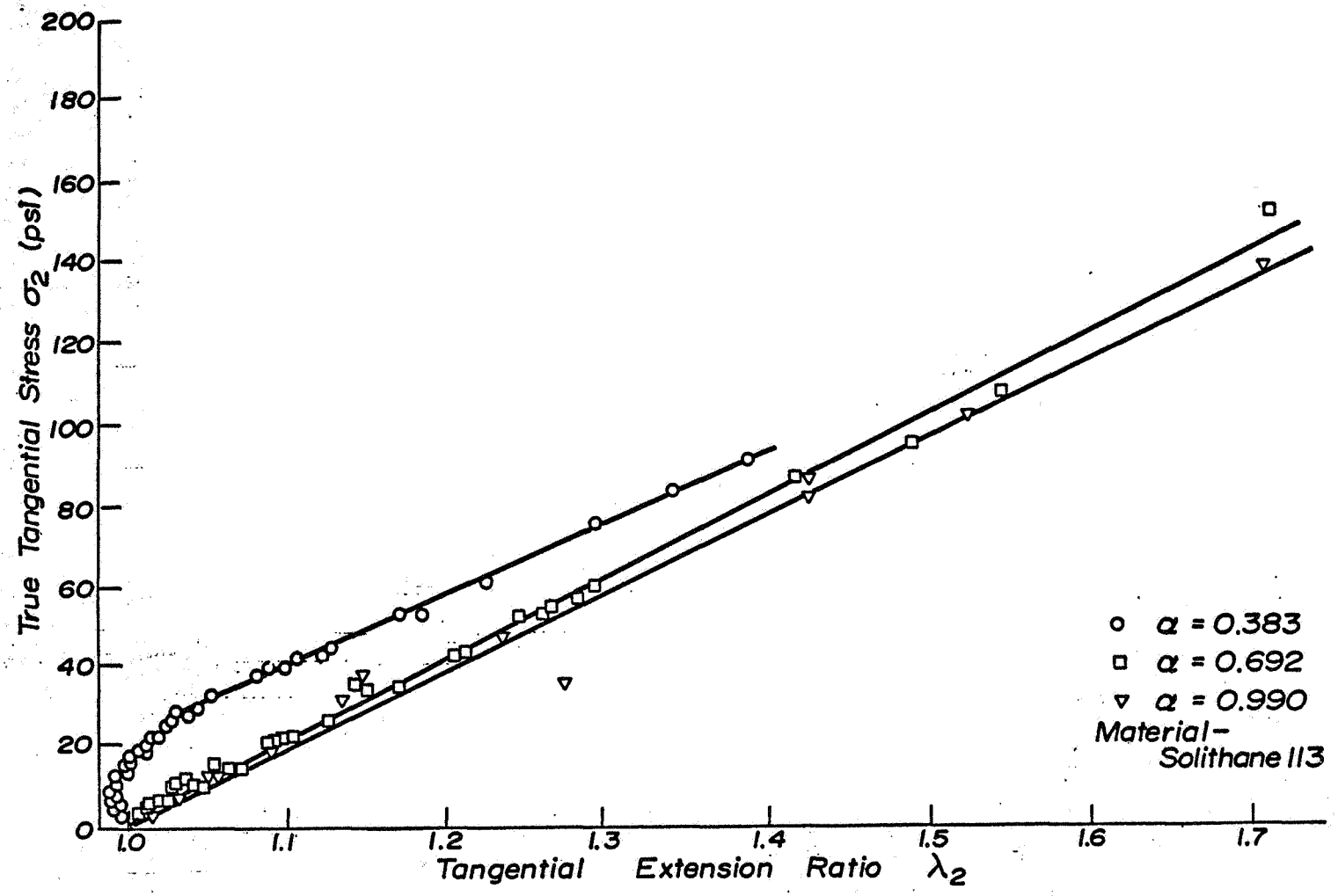

Figure 6. True Tangential Stress Versus Tangential Extension Ratio Curves for Solithane 113 Under Biaxial Loading.

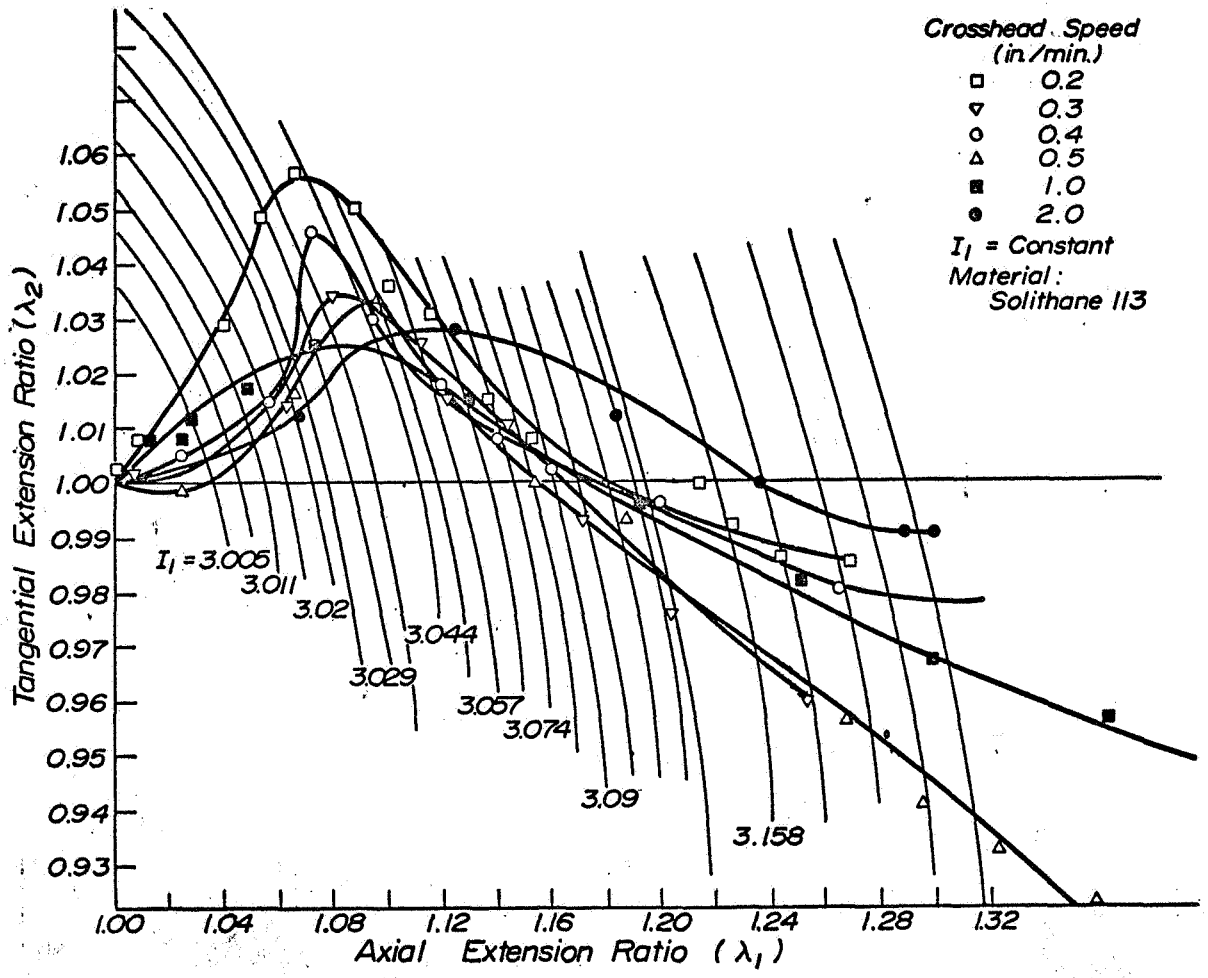

Figure 7. Tangential Extension Ratio λ_2 Versus Axial Extension Ratio λ_1 Curves Obtained from Biaxial Stress Experiments

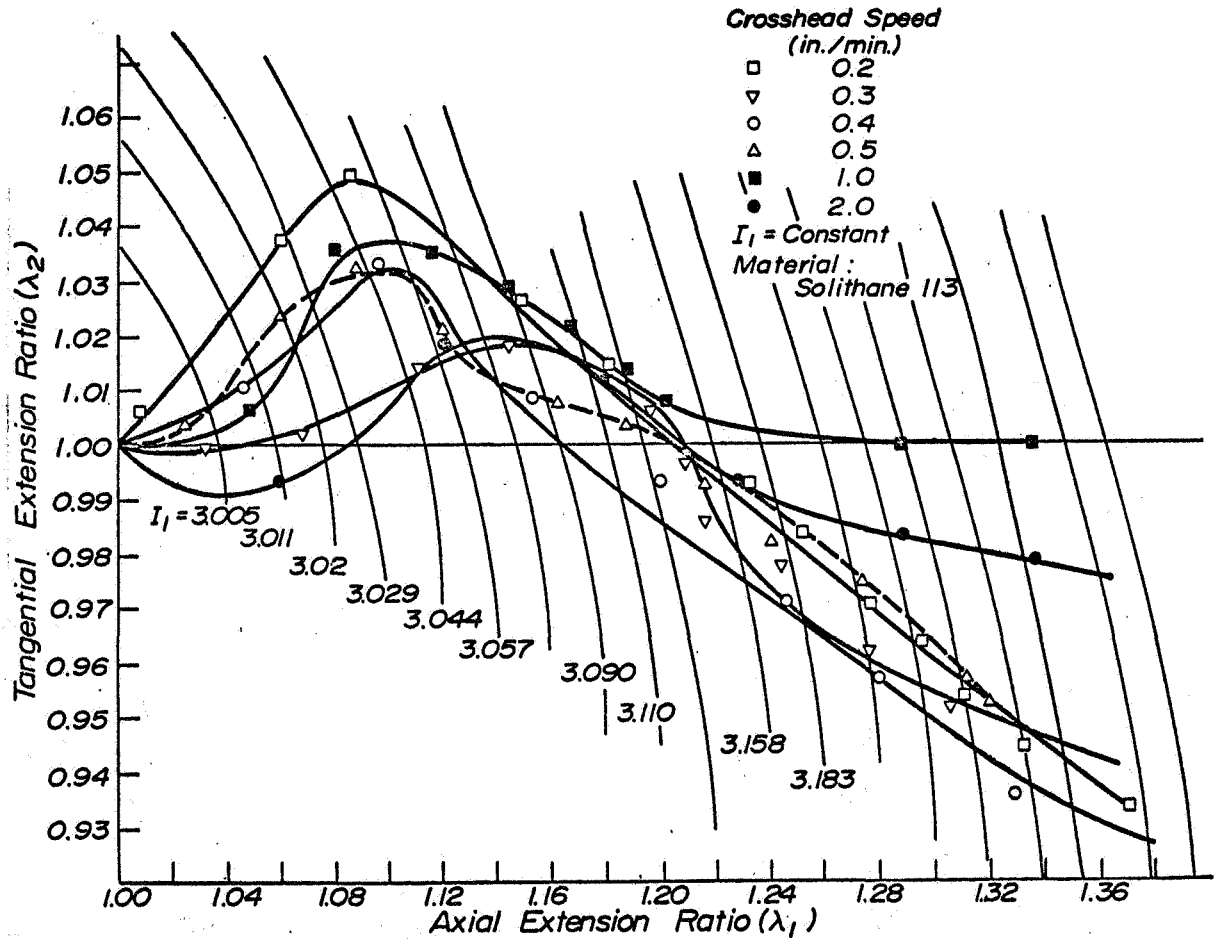

Figure 8. Tangential Extension Ratio λ_2 Versus Axial Extension Ratio λ_1 Curves Obtained from Biaxial Stress Experiment

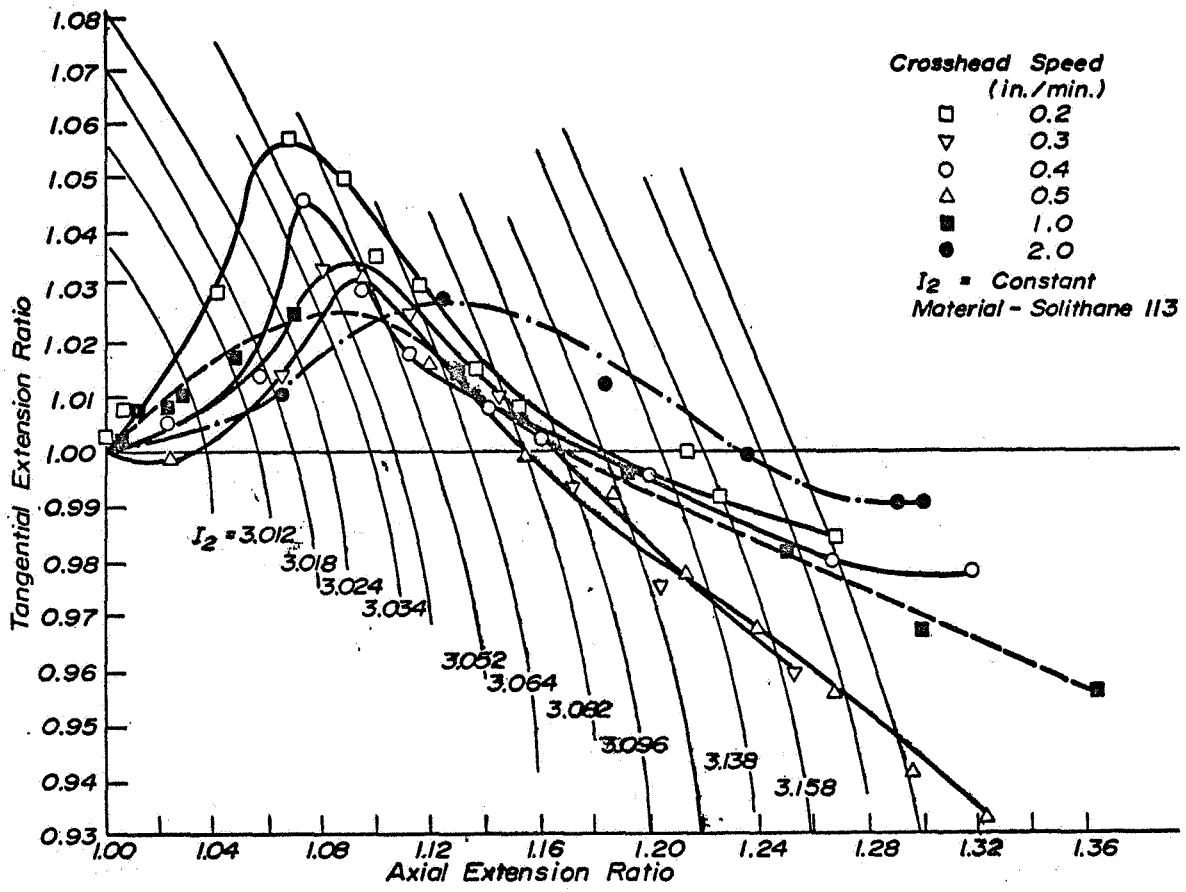

Figure 9. Tangential Extension Ratio λ_2 Versus Axial Extension Ratio λ_1 Curves Obtained from Biaxial Stress Experiments

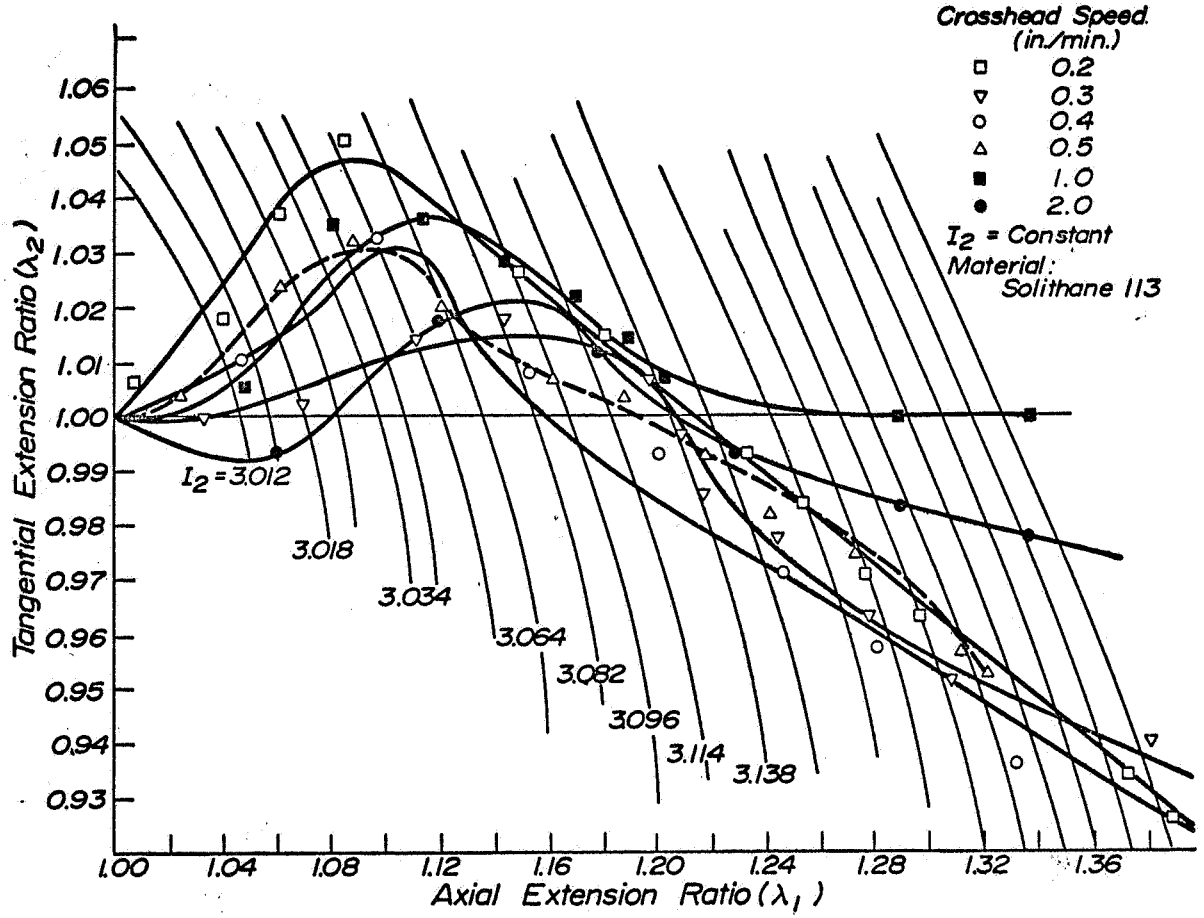

Figure 10. Tangential Extension Ratio λ_2 Versus Axial Extension Ratio λ_1 Curves Obtained from Biaxial Stress Experiment

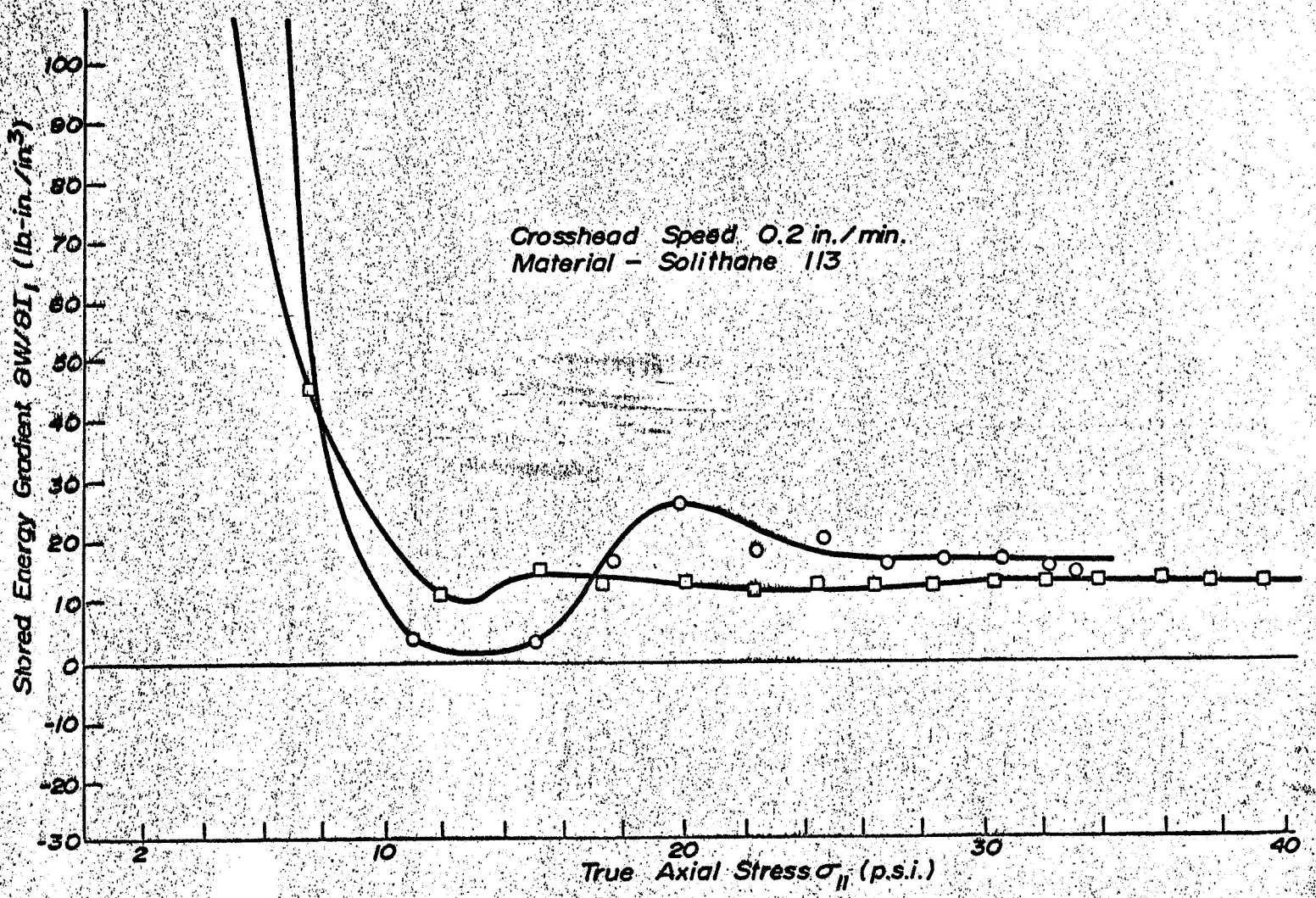

Figure 11. Stored Energy Gradient with Respect to I_1 Versus True Axial Stress

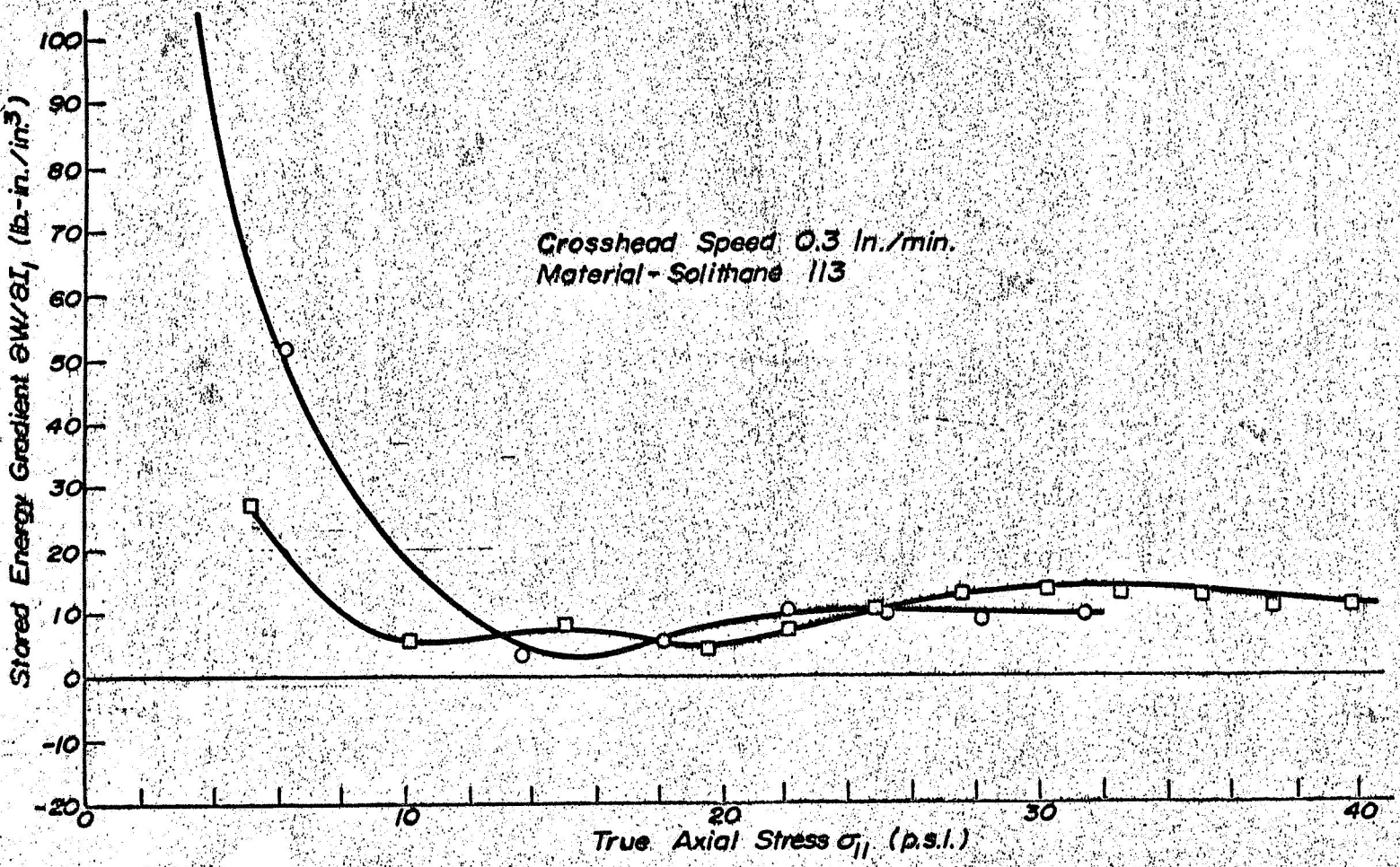

Figure 12. Stored Energy Gradient with Respect to I_1 Versus True Axial Stress

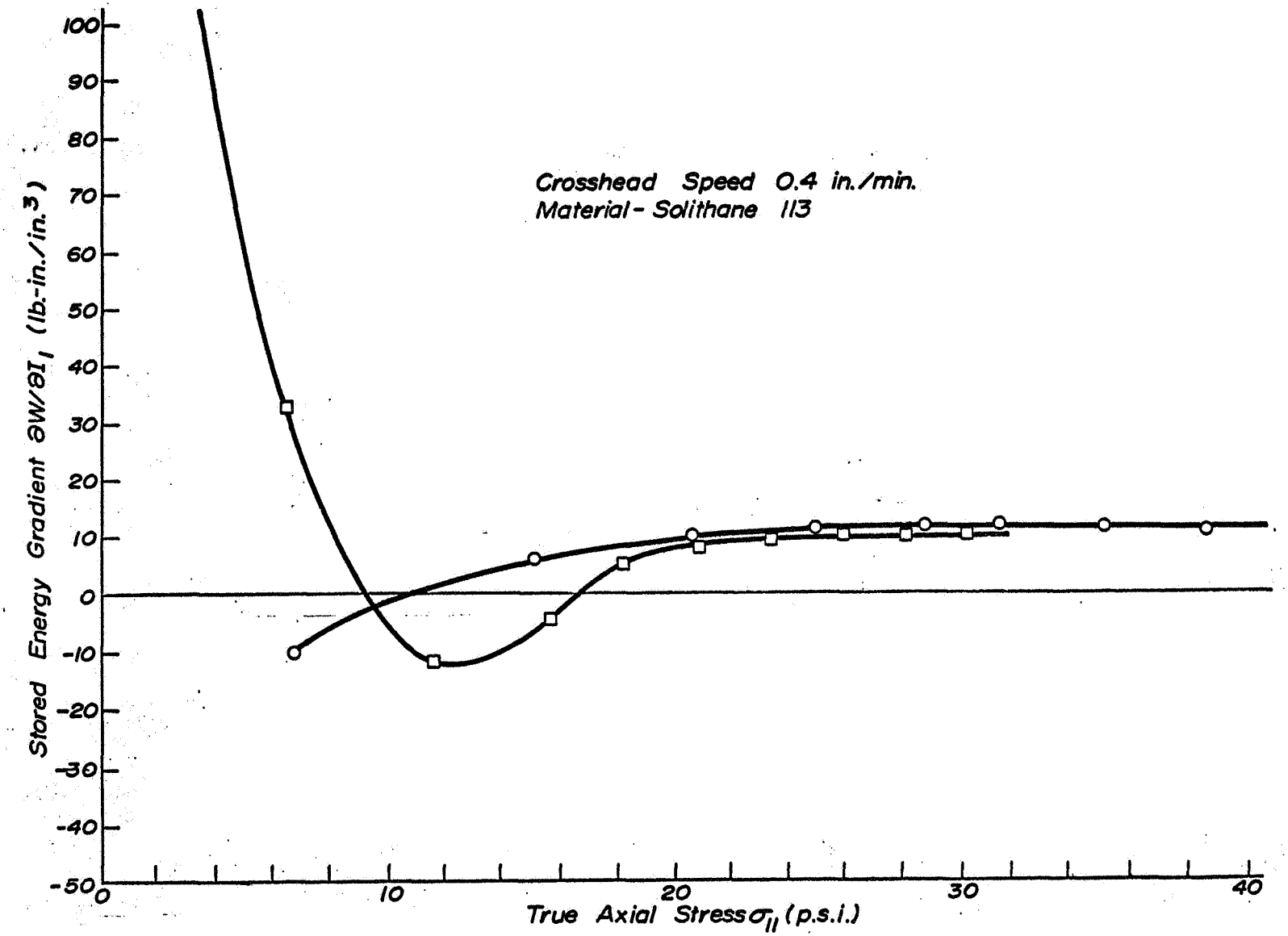

Figure 13. Stored Energy Gradient with Respect to I_1 Versus True Axial Stress

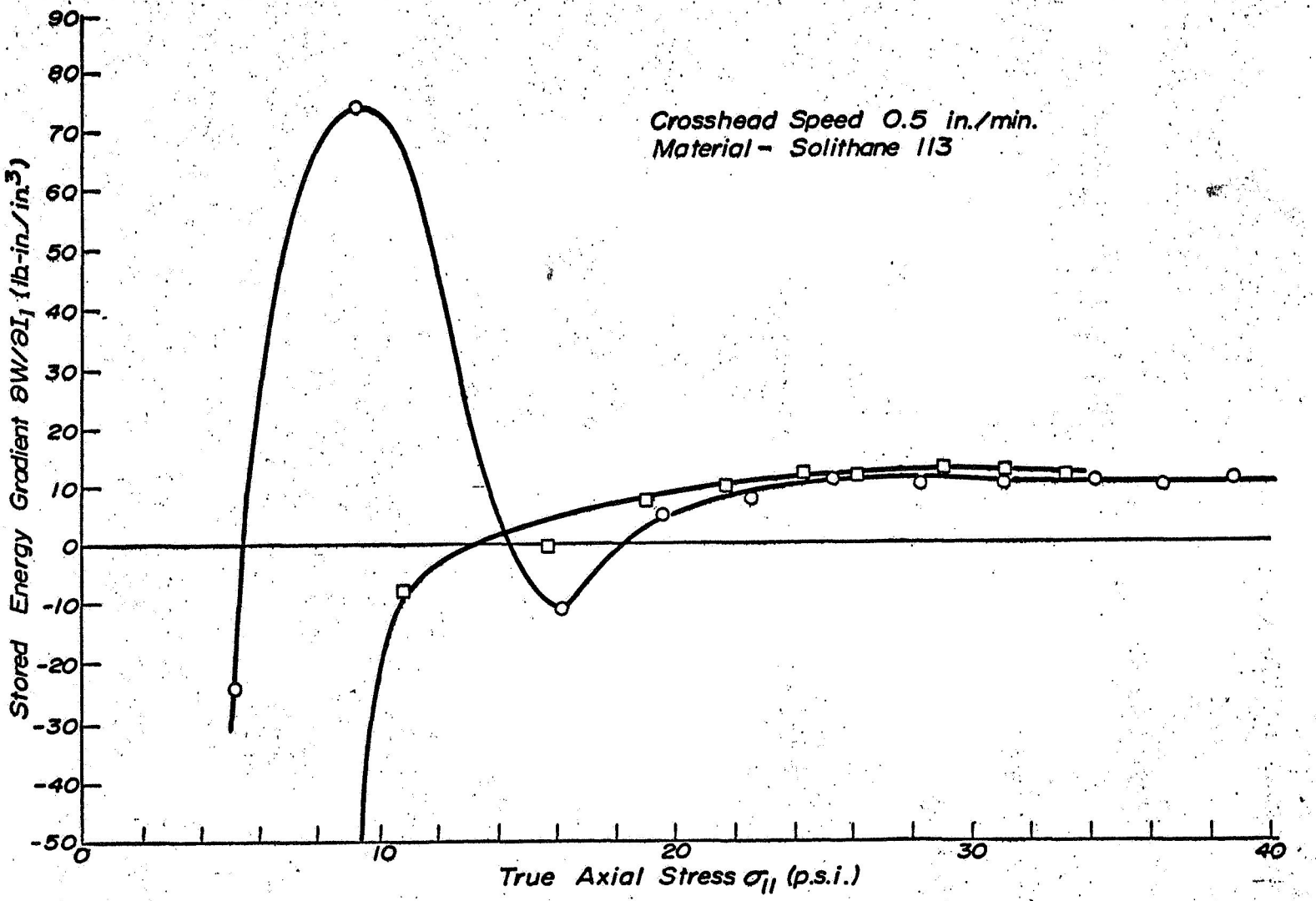

Figure 14. Stored Energy Gradient with Respect to I_1 Versus True Axial Stress

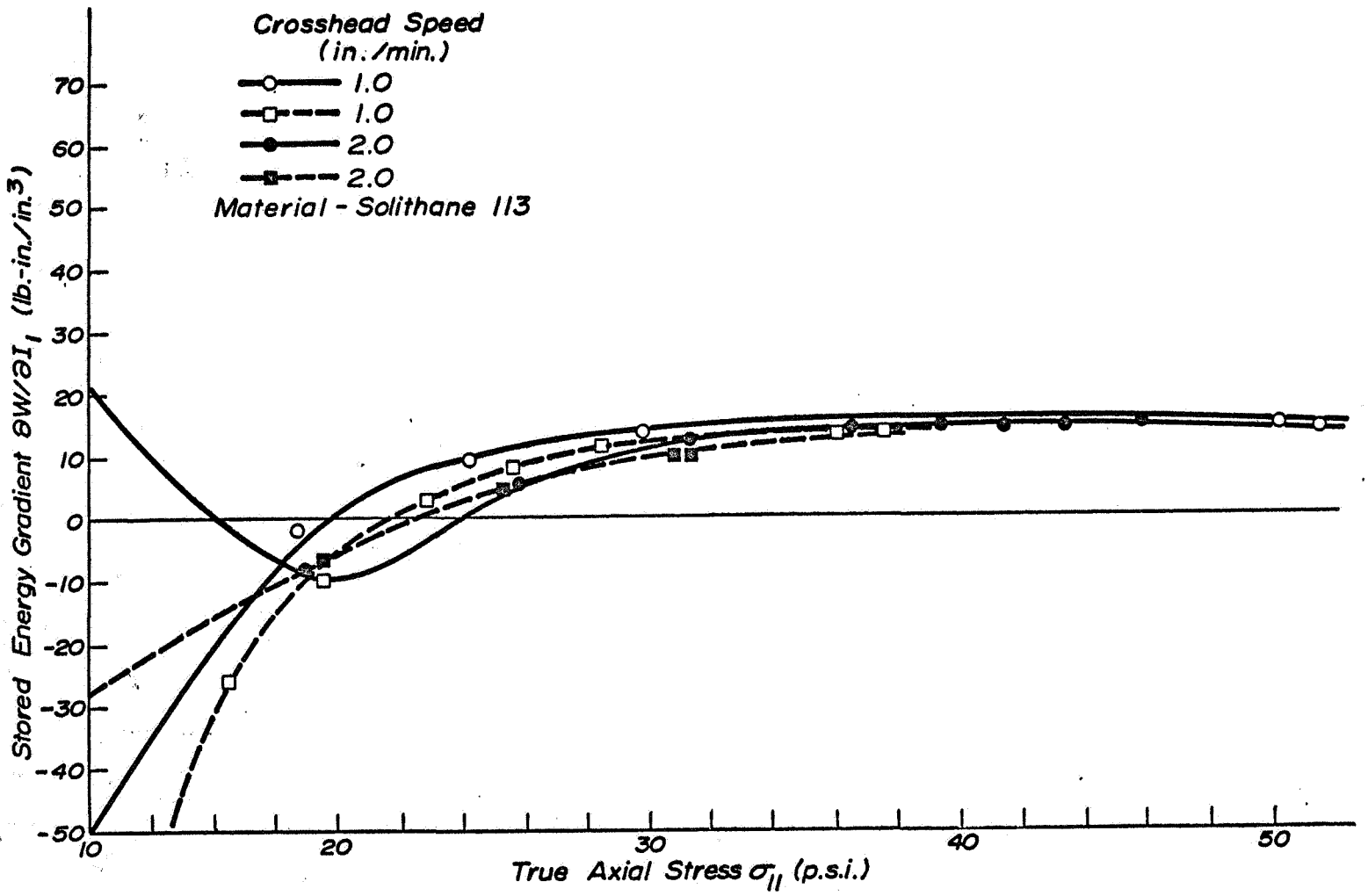

Figure 15. Stored Energy Gradient with Respect to I_1 Versus True Axial Stress

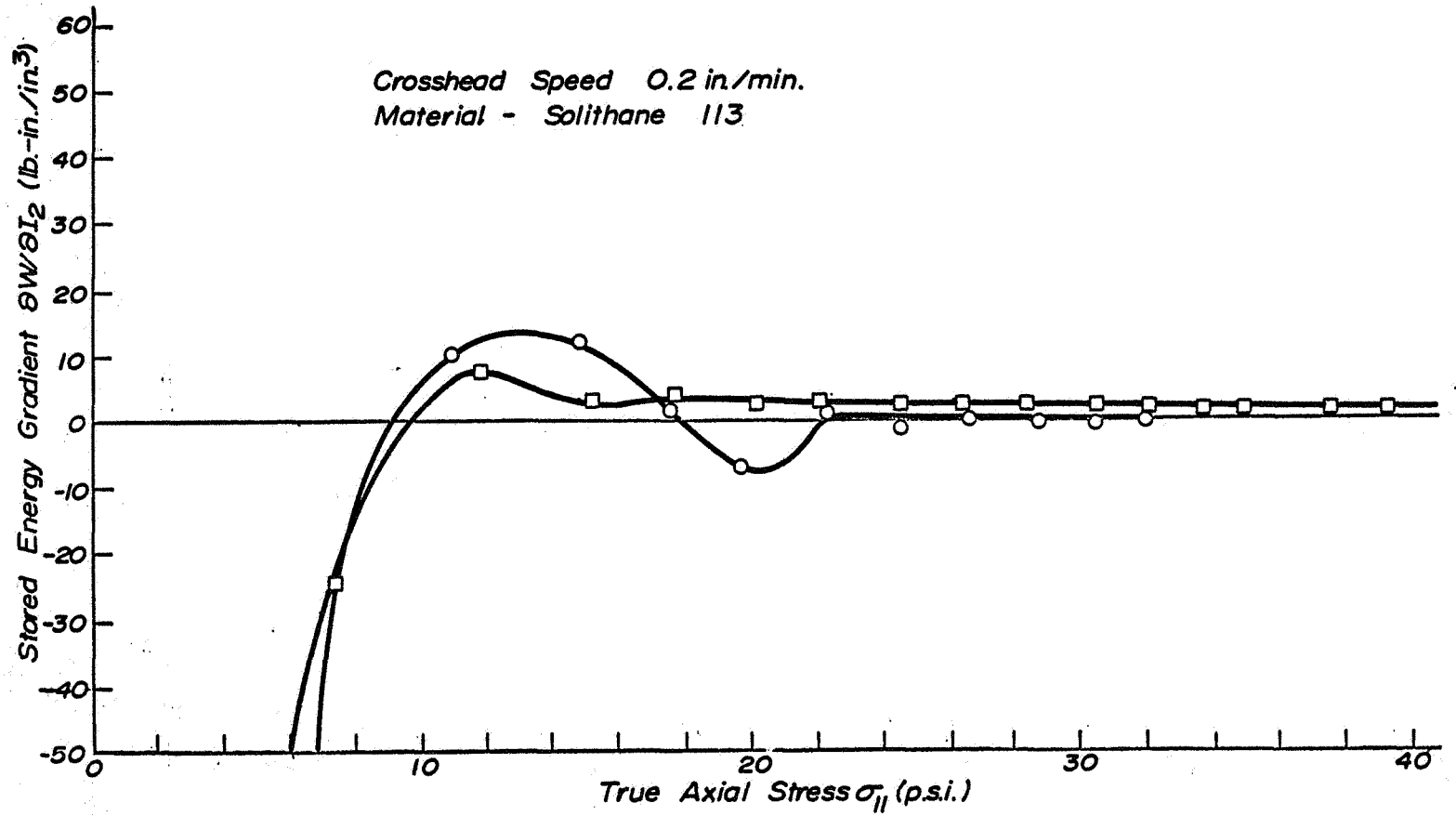

Figure 16. Stored Energy Gradient with Respect to I_2 Versus True Axial Stress

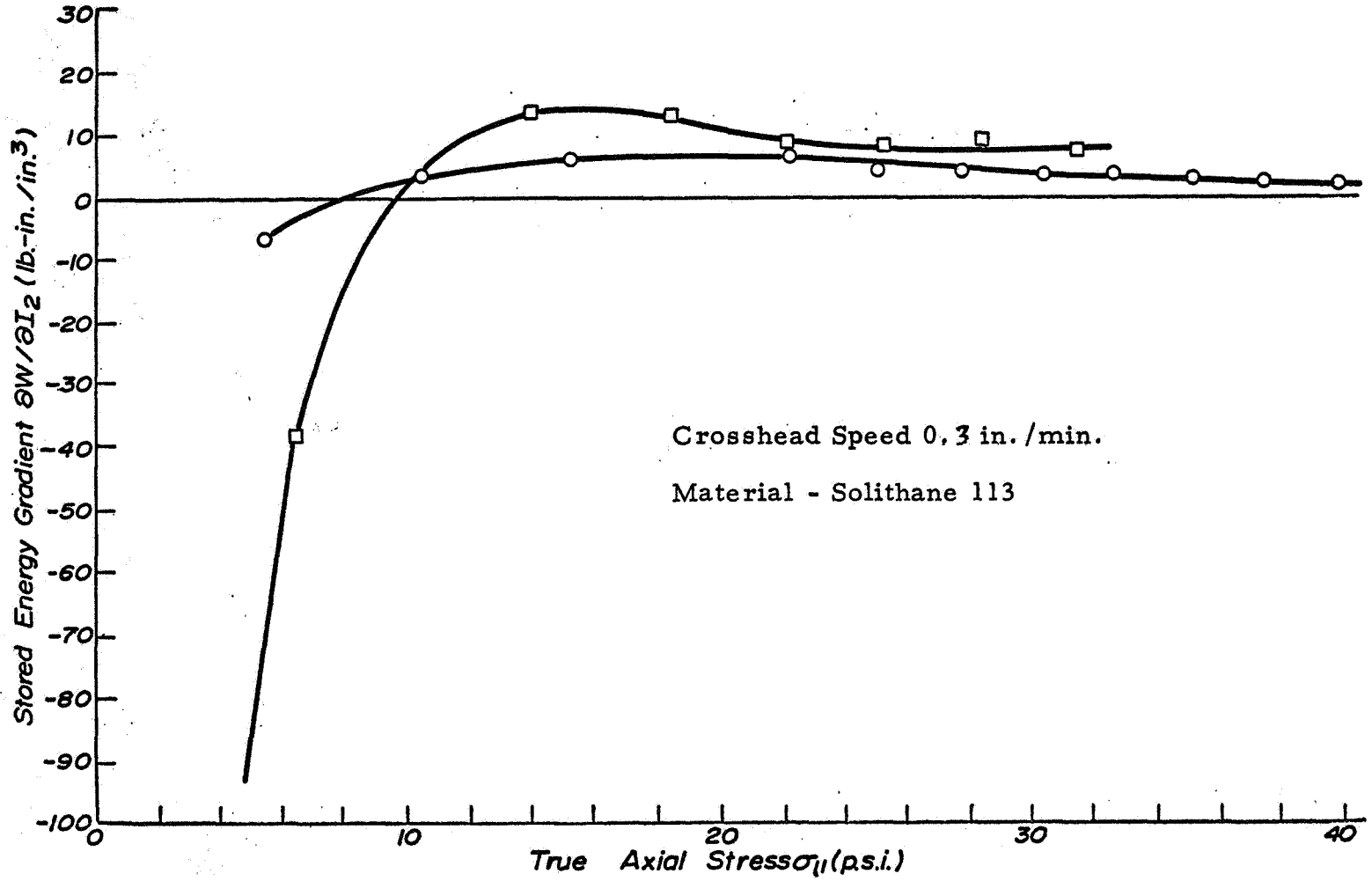

Figure 17. Stored Energy Gradient with Respect to I_2 Versus True Axial Stress

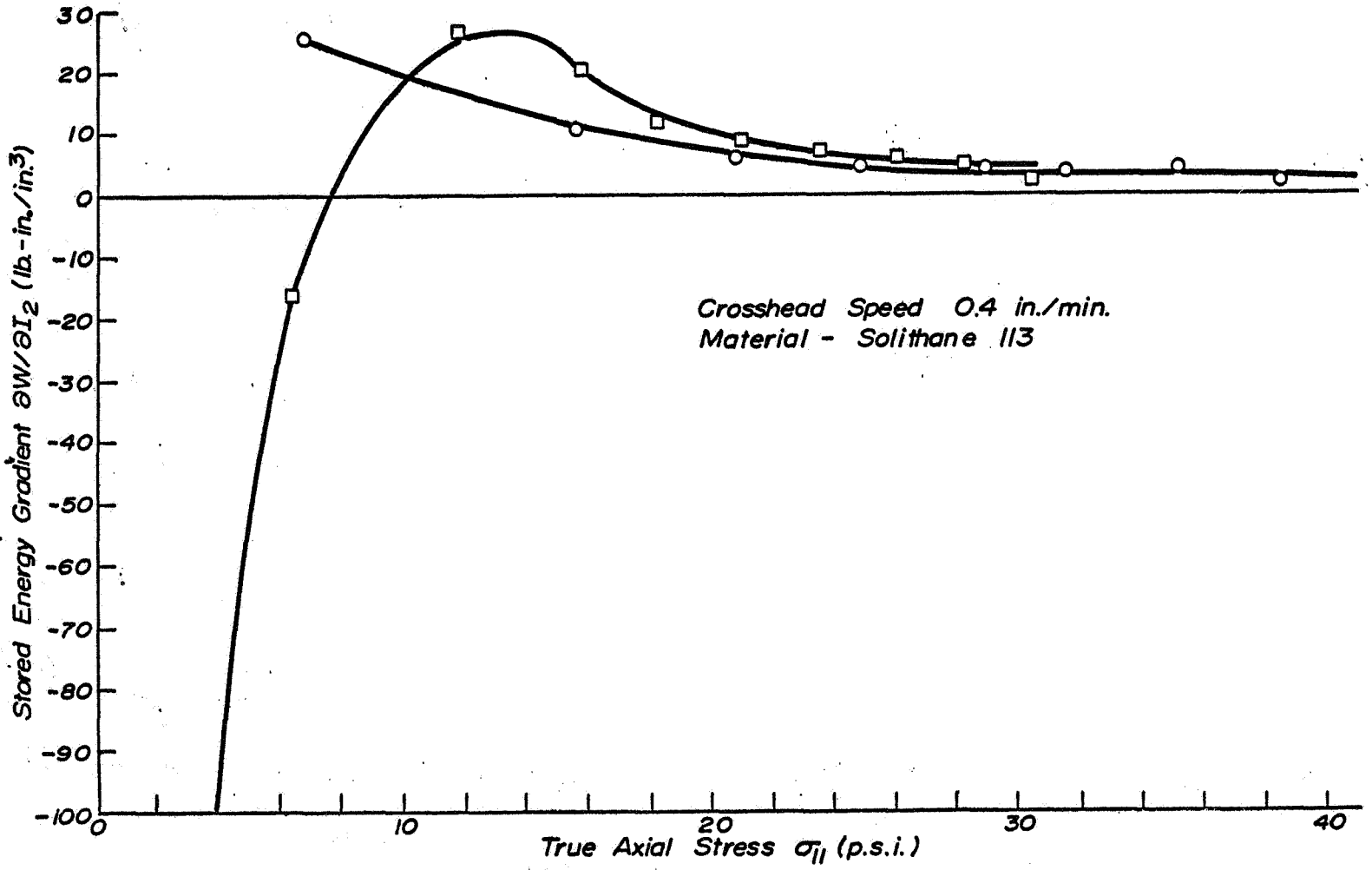

Figure 18. Stored Energy Gradient with Respect to I_2 Versus True Axial Stress

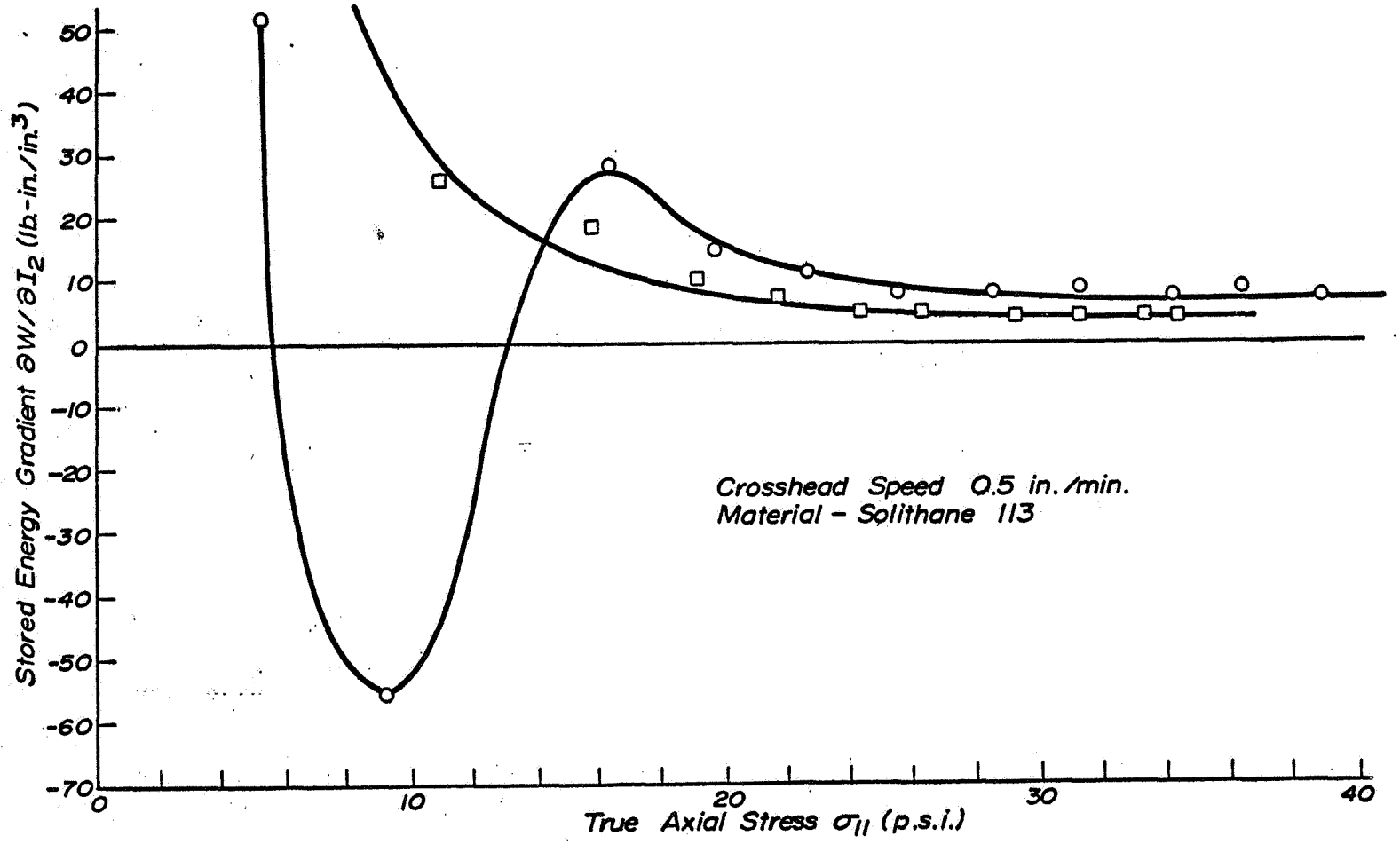

Figure 19. Stored Energy Gradient with Respect to I_2 Versus True Axial Stress

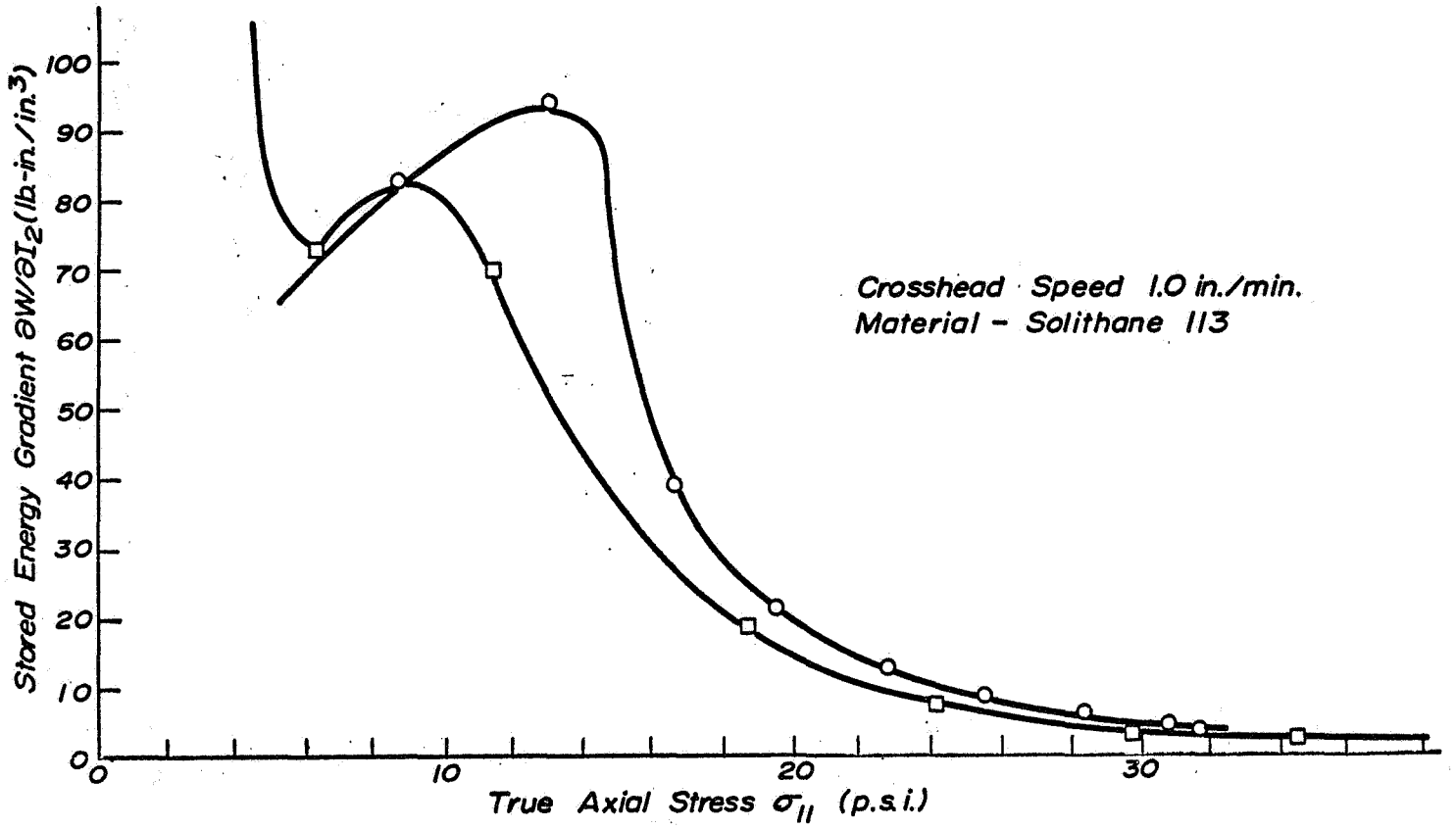

Figure 20. Stored Energy Gradient with Respect to I_2 Versus True Axial Stress

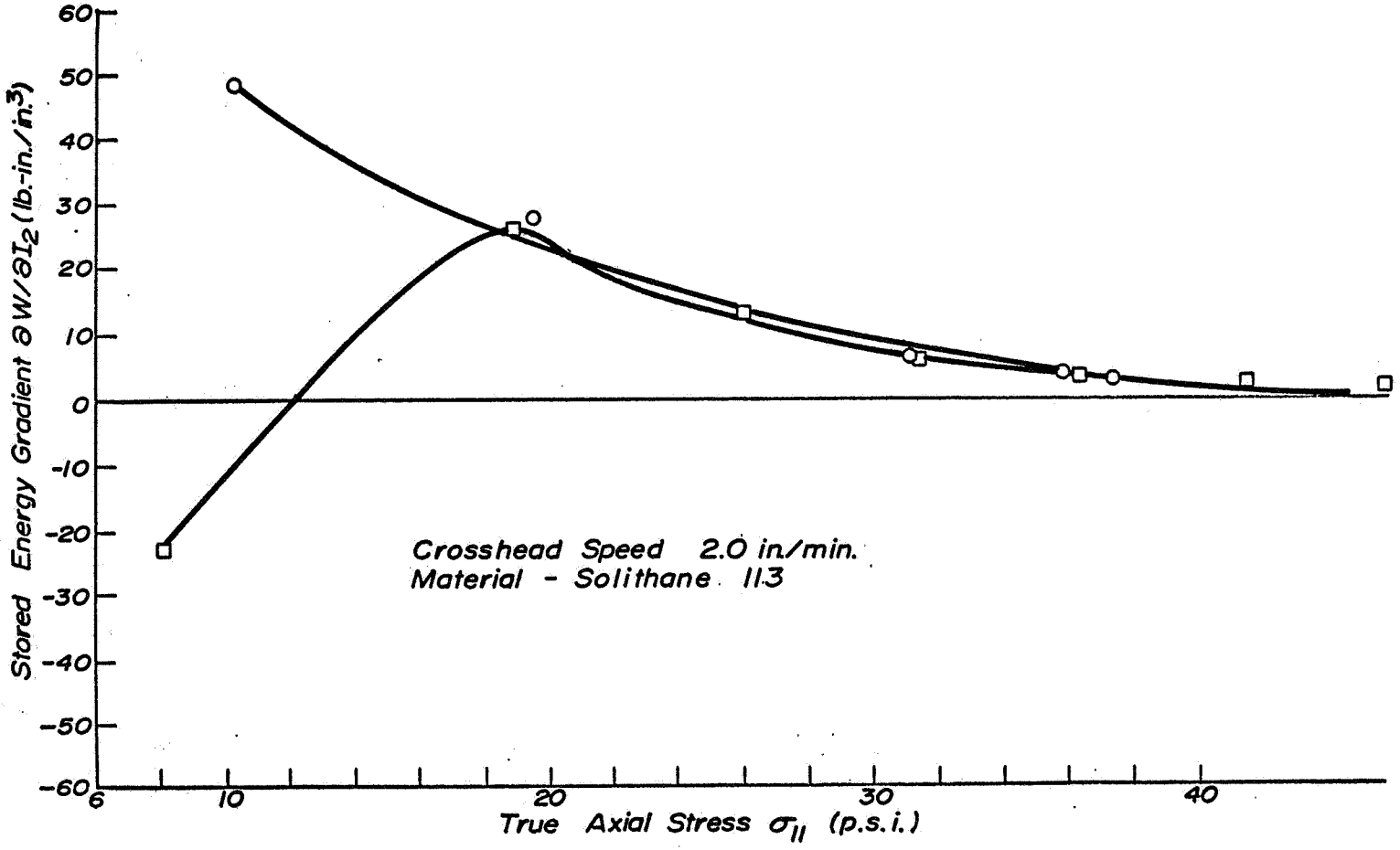

Figure 21. Stored Energy Gradient with Respect to I_2 Versus True Axial Stress

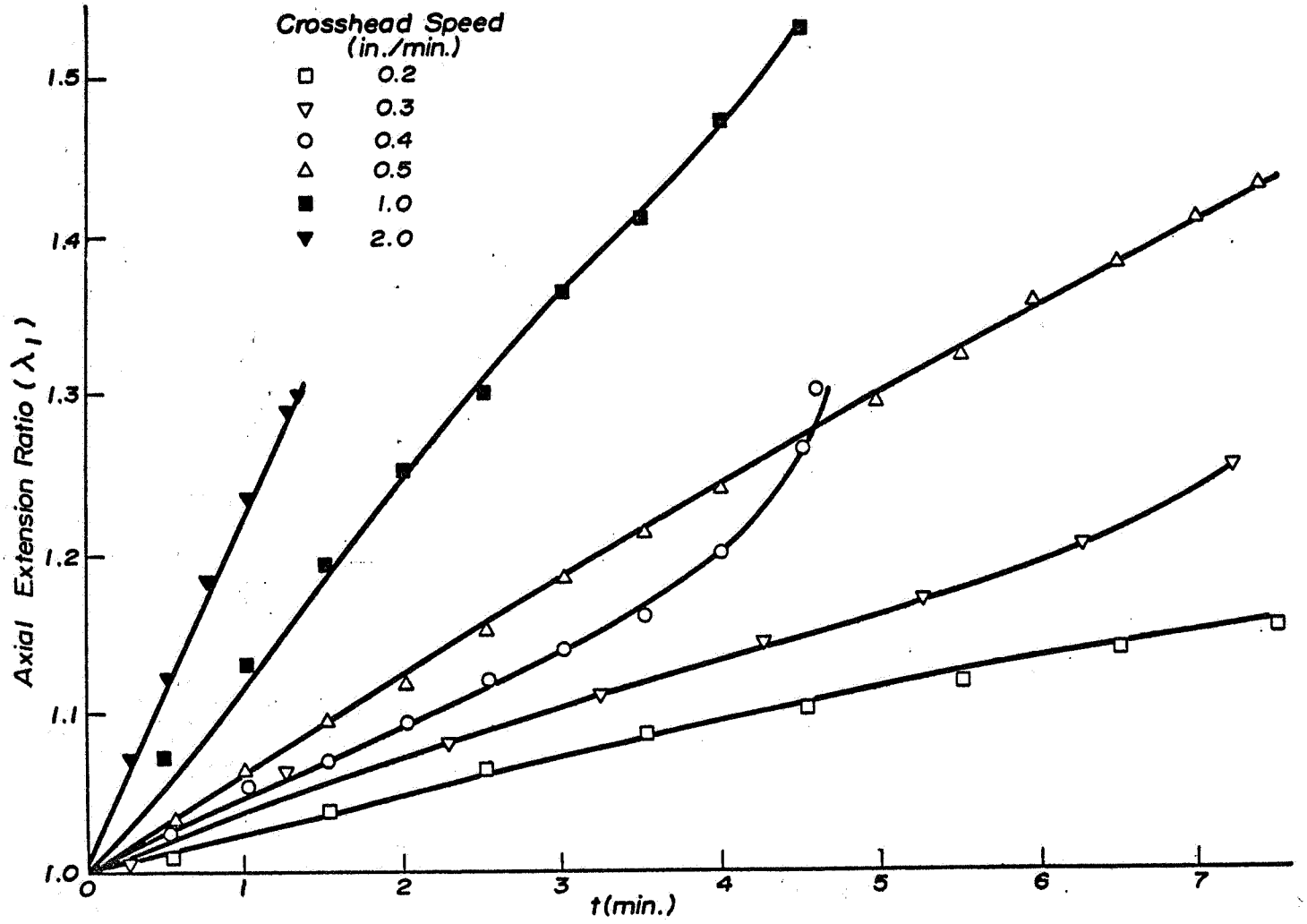

Figure 22. Axial Extension Ratio λ_1 Versus Time

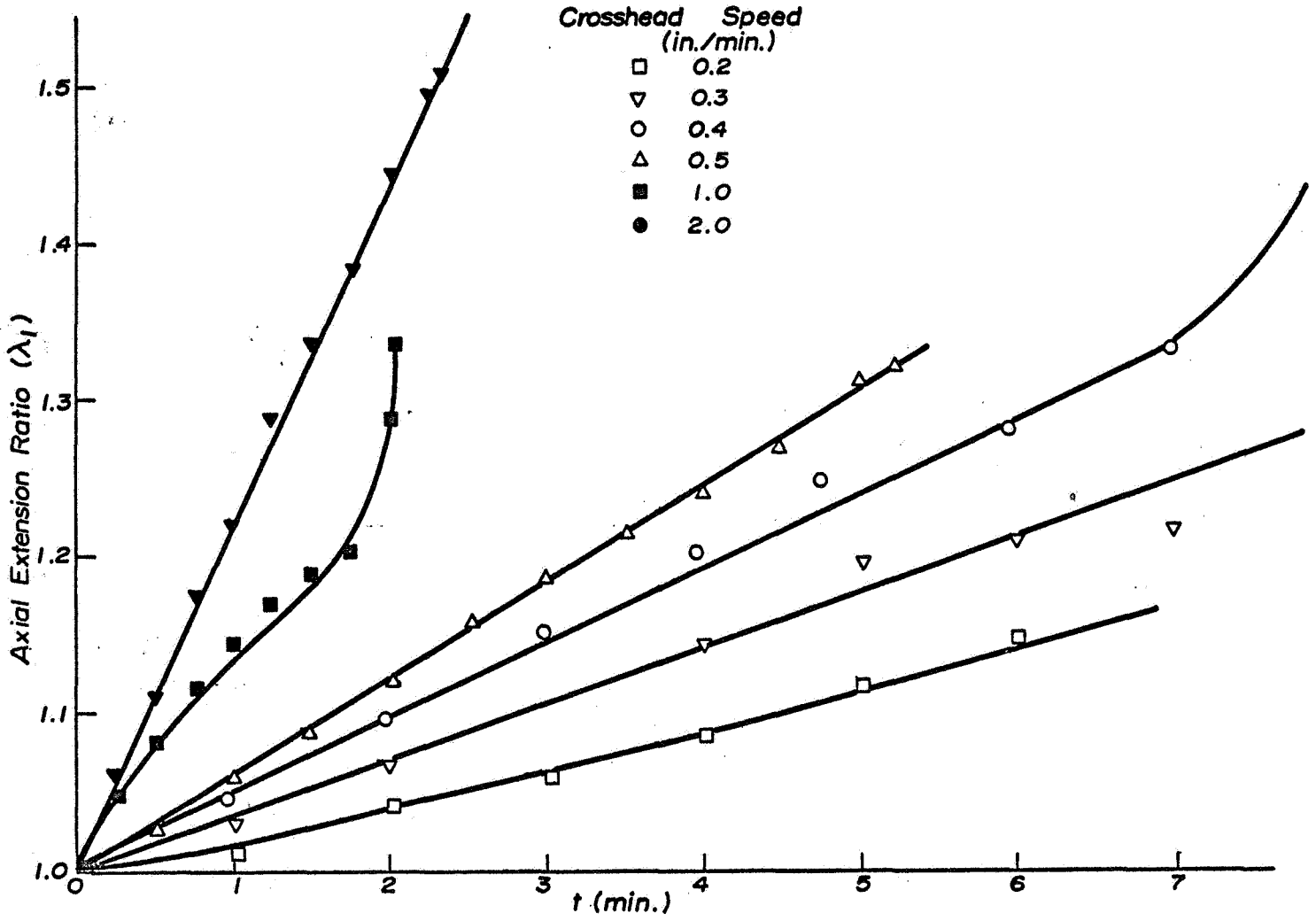

Figure 23. Axial Extension Ratio λ_1 Versus Time

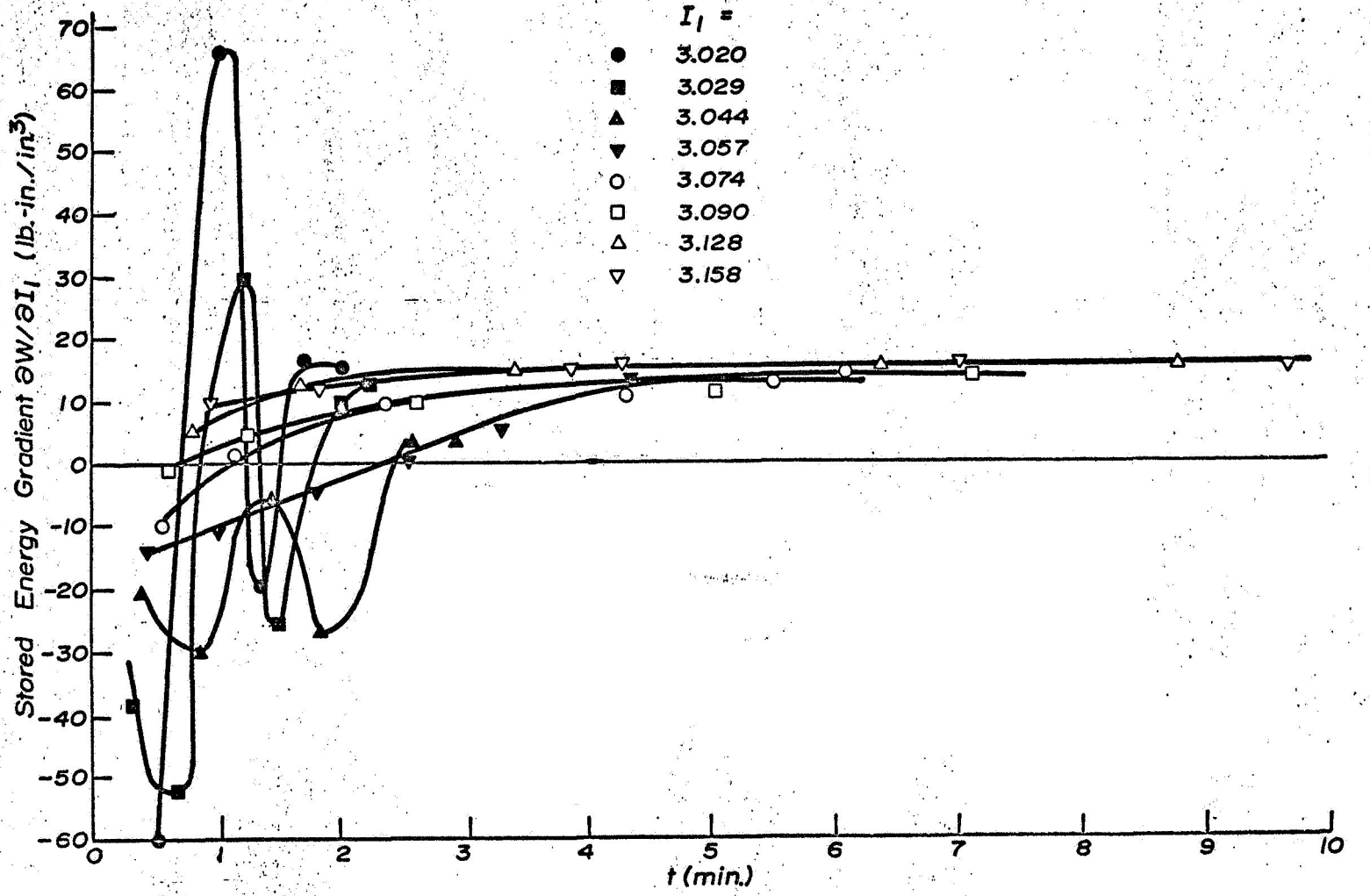

Figure 24. Stored Energy Gradient $\frac{\partial w}{\partial I_1}$ Versus Time at Given I_1
(First Test)

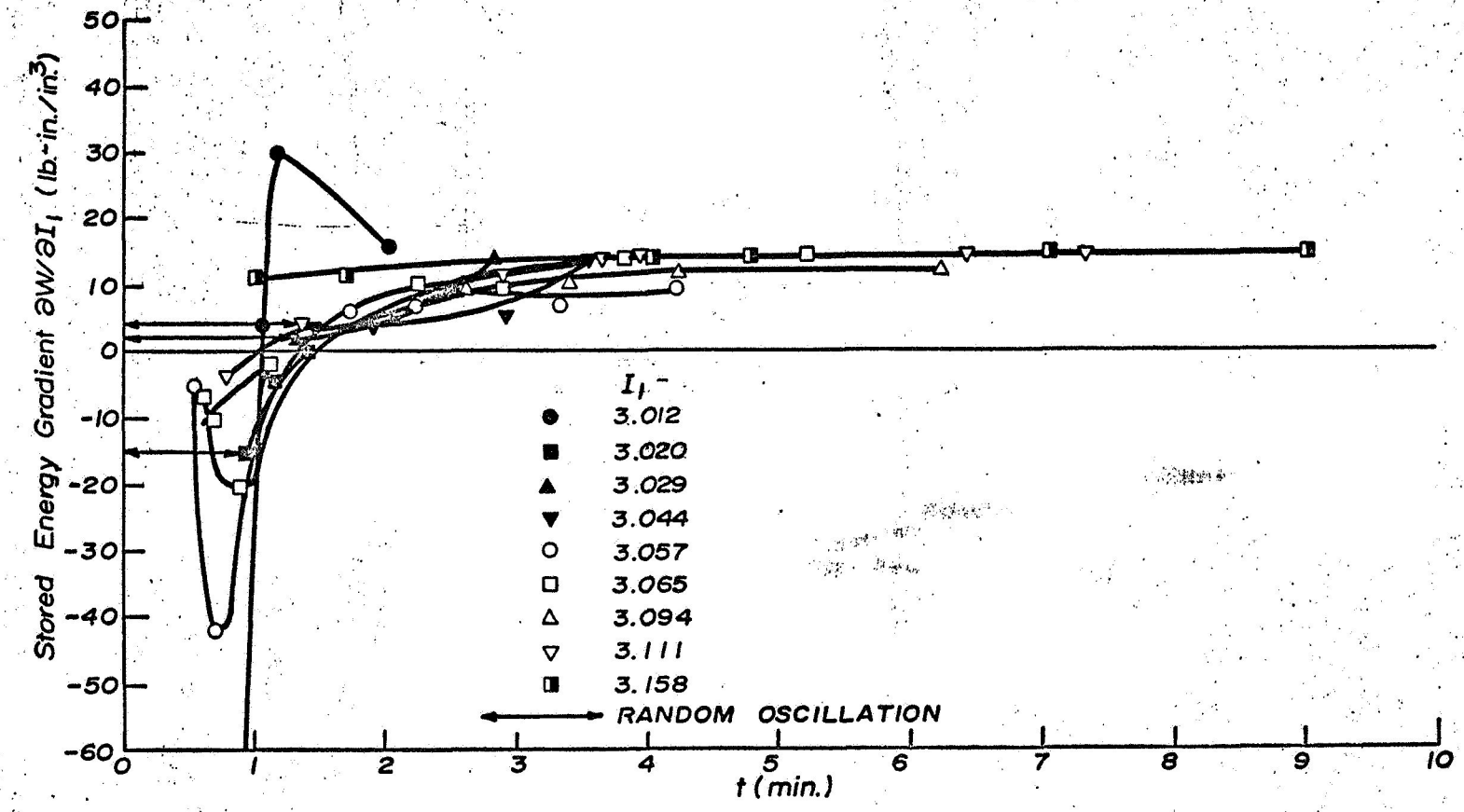

Figure 25. Stored Energy Gradient $\frac{\partial w}{\partial I_1}$ Versus Time at Given I_1
(Second Test)

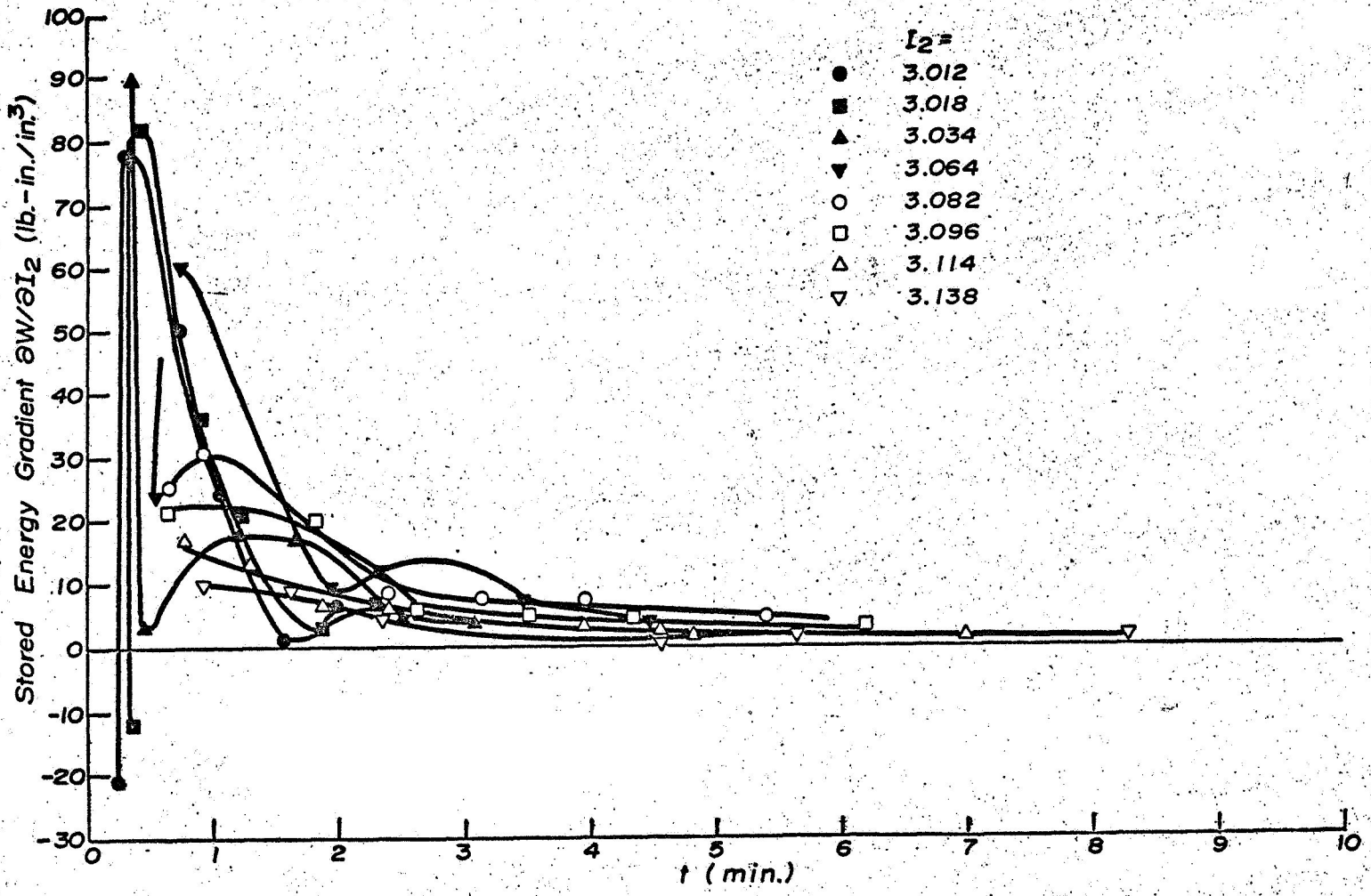

Figure 26. Stored Energy Gradient $\frac{\partial w}{\partial I_2}$ Versus Time at Given I_2

(Second Test)

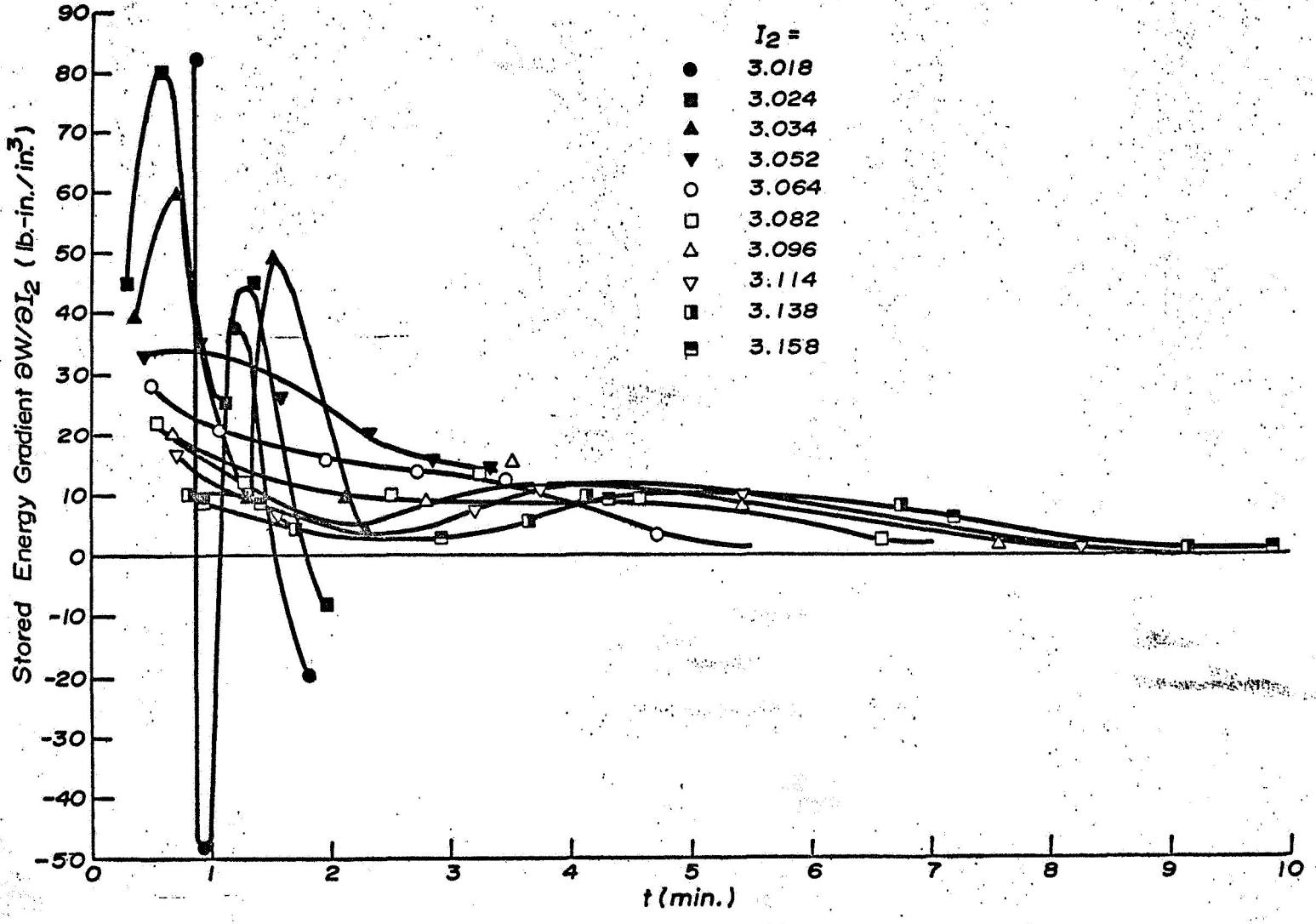

Figure 27. Stored Energy Gradient $\frac{\partial w}{\partial I_2}$ Versus Time at Given I_2
(First Test)

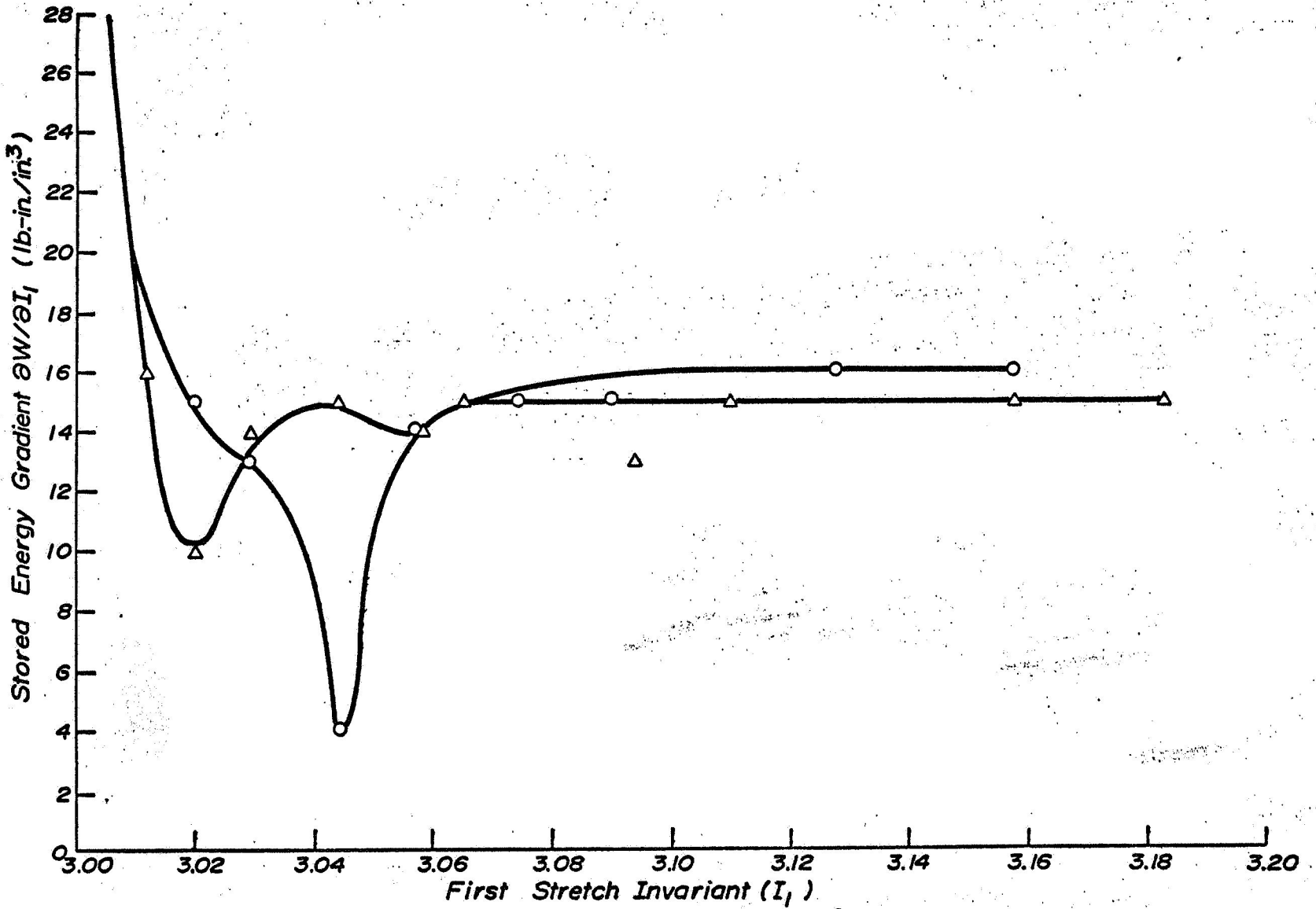

Figure 28. Variation of Stored Energy Gradient $\frac{\partial w}{\partial I_1}$ with the First Stretch Invariant I_1 (Strain Rate is Controlled)

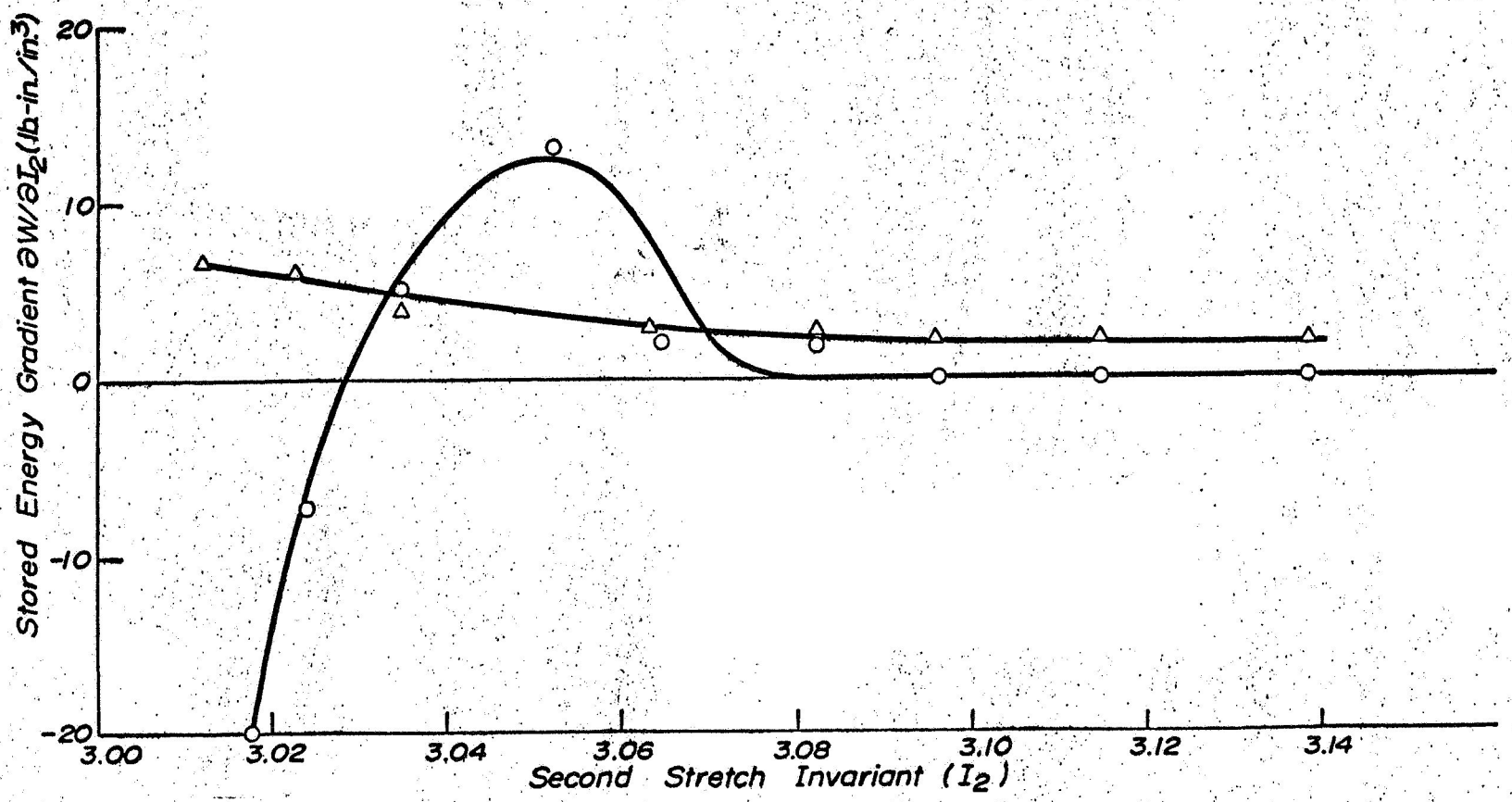

Figure 29. Variation of Stored Energy Gradient $\frac{\partial w}{\partial I_2}$ with the Second Stretch Invarient I_2 (Strain Rate is Controlled)

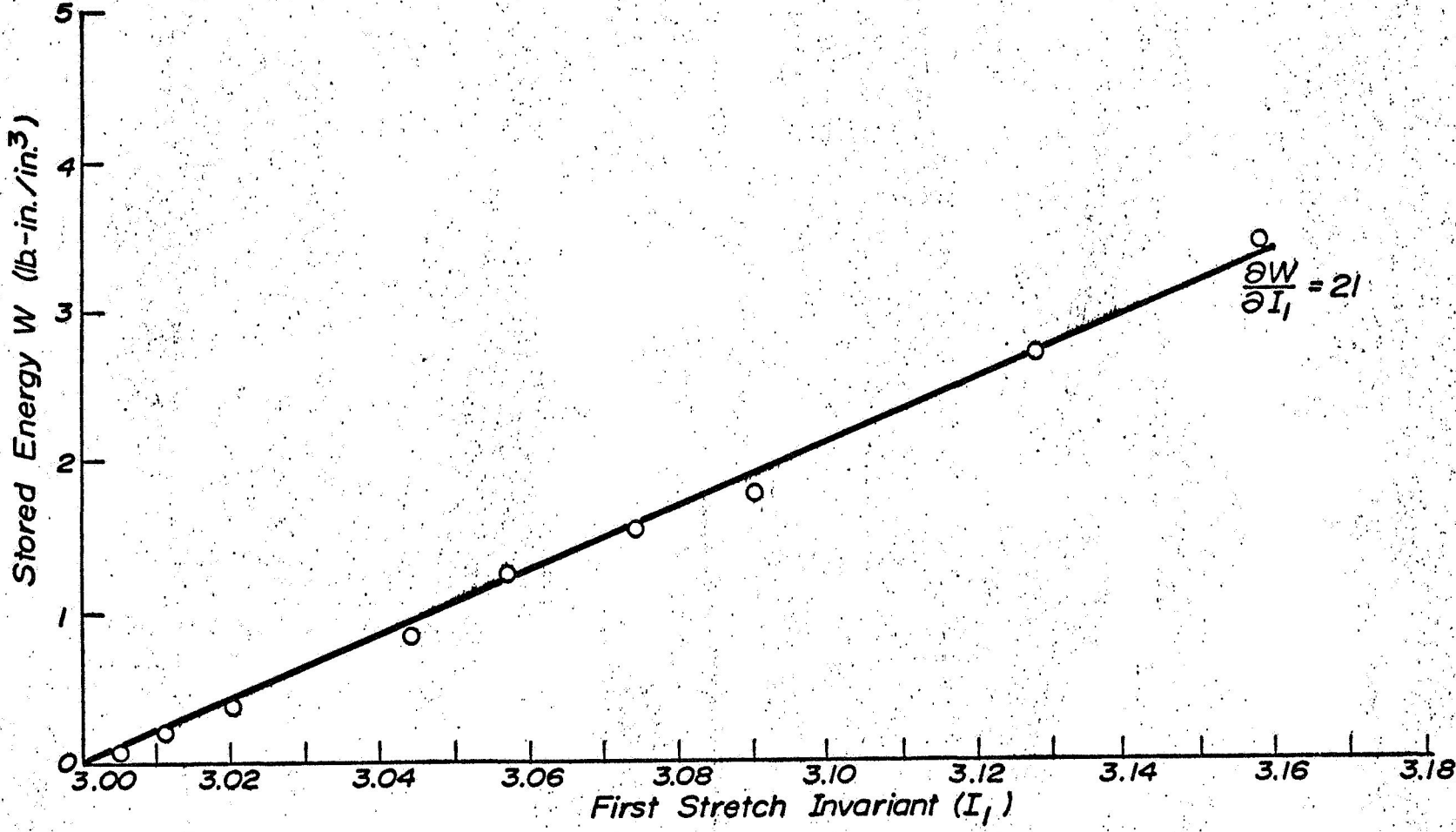

Figure 30. Stored Energy Versus First Stretch Invariant I_1 (Strain Rate is Controlled)

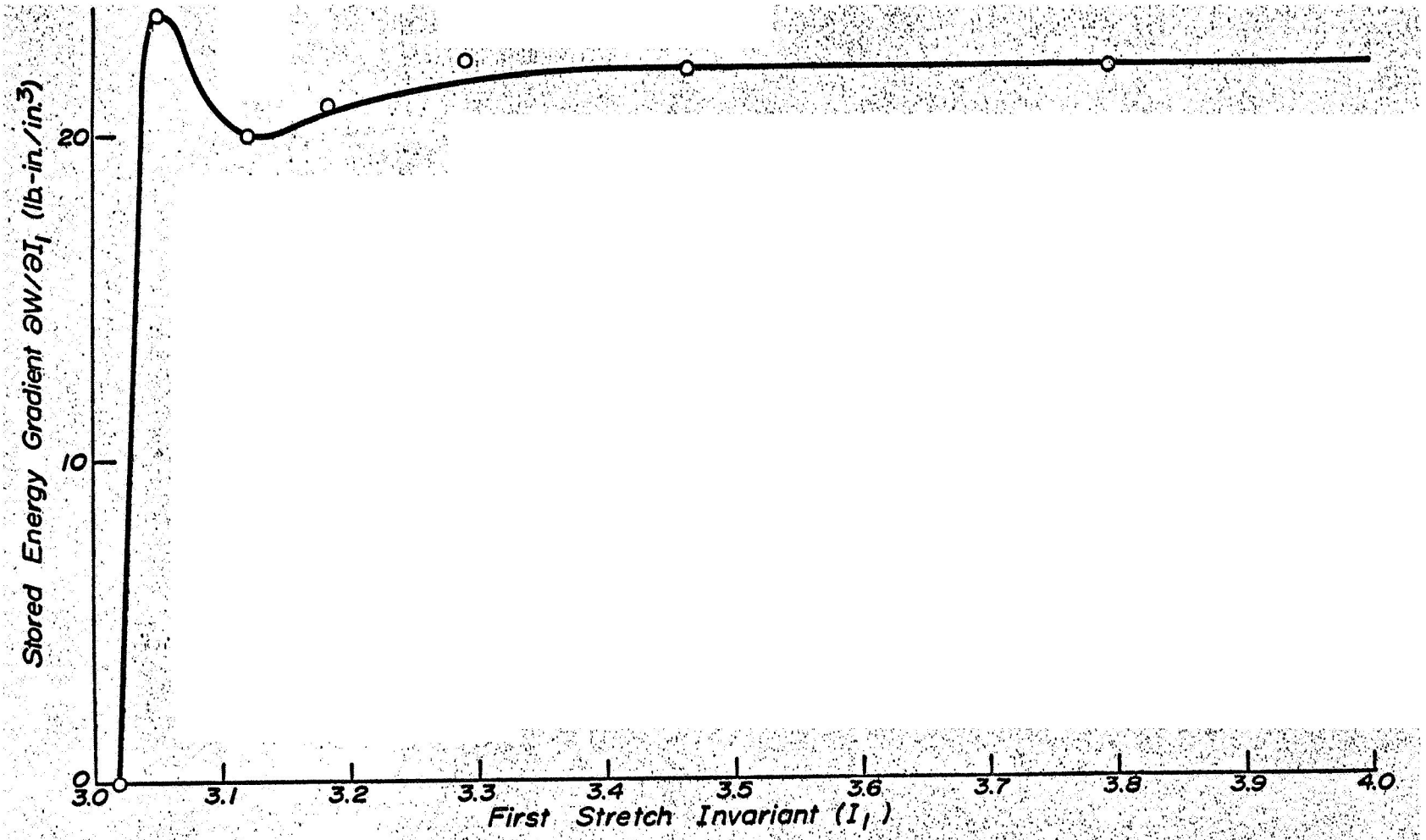

Figure 31. Variation of Stored Energy Gradient $\frac{\partial w}{\partial I_1}$ with the First Stretch Invarient I_1 (Stress Rate is Controlled).

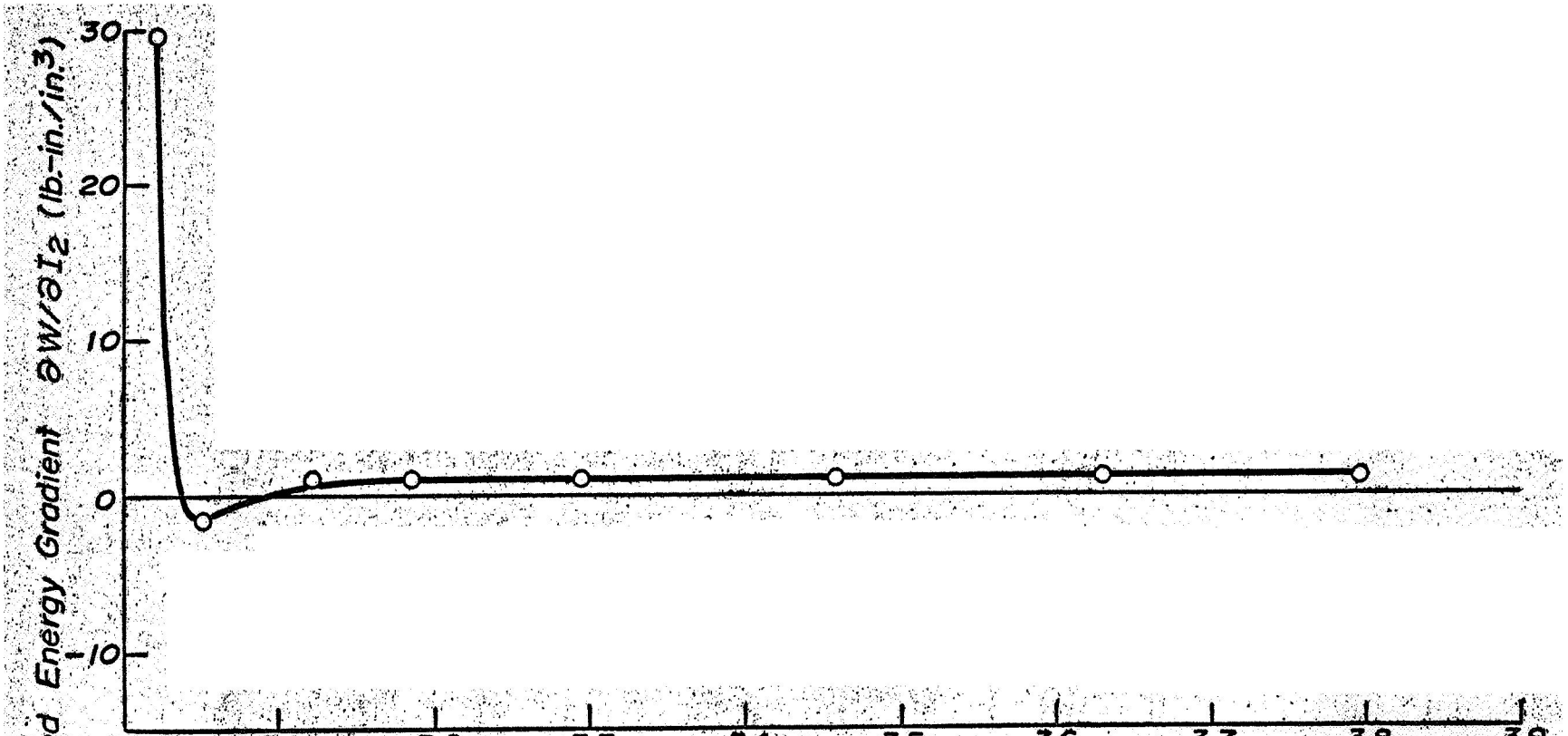

Figure 32. Variation of Stored Energy Gradient $\frac{\partial w}{\partial I_2}$ with the Second Stretch Invarient I_2 (Stress Rate is Controlled)